RECONSTRUCTION OF HOLOCENE ENVIRONMENTAL CHANGES IN NORTHERN BRITISH COLUMBIA USING FOSSIL MIDGES

by

Erin Mattea Fleming

B.Sc., Okanagan University College, 2005

A THESIS SUBMITTED IN PARTIAL FULFILLMENT OF
THE REQUIREMENTS FOR THE DEGREE OF

MASTER OF SCIENCE

in

The College of Graduate Studies

(Environmental Science)

UNIVERSITY OF BRITISH COLUMBIA

(Okanagan)

August 2008

ABSTRACT

Lake sediments contain the remains of midge communities that may be used as biological proxies for inferring past environmental changes. Freshwater midges, including Chironomidae and Chaoboridae, from two alpine tarns (Pyramid Lake and Bullwinkle Lake) in the Cassiar Mountains of northern British Columbia were used to estimate Holocene palaeotemperature changes, and more specifically, to test for the presence of the Milankovitch thermal maximum, an early Holocene warm interval coinciding with peak Holocene summer solar insolation. Mean July air temperatures were reconstructed using midge-inference models developed via weighted averaging-partial least squares (WA-PLS) regression. Cold-tolerant midge taxa dominate the stratigraphies from both Pyramid and Bullwinkle Lakes; however, warm-adapted species are more common in Bullwinkle Lake. Early Holocene warming is apparent at both lakes, however it is unclear whether this is indicative of the Milankovitch thermal maximum. A decrease in temperature occurs from 8,700-7,900 cal. yr BP at Pyramid Lake, around the same time that the 8,200 cal. yr BP cooling event occurred in the northern hemisphere. During the middle Holocene, records from Pyramid Lake indicate an overall decrease in temperature, with a short period of warmer temperatures that peak at 5,100 cal. yr BP. Temperatures fluctuate little during this time at Bullwinkle Lake. A short warming phase is apparent at both lakes during the late Holocene. July temperatures are highest at 2,000 cal. yr BP (10.5°C) in Pyramid Lake and at 1,200 cal. yr BP (13°C) in Bullwinkle Lake. Thereafter, temperatures return to what they were before the warming occurred, and at Bullwinkle Lake, vary little throughout the remainder of the Holocene.

TABLE OF CONTENTS

LIST OF TABLES

LIST OF FIGURES

ACKNOWLEDGEMENTS

I would like to extend a sincere thank-you to the following people for their invaluable contributions, guidance and support all through this exciting journey:

- Ian Walker
- Robert Young
- Robert Lalonde
- Erin Barley
- Lydia Stepanovic
- David Mazzucchi
- Christina Bleskie
- Marianne Chase
- Heather Gray
- Kimberly Loudon
- Peter Rotheisler
- Alice Telka
- Duane Froese
- Jerry Osborn
- Douglas Hallett
- Skye Thomson

DEDICATION

To my parents, Terry and Arlene Fleming,

for their endless love and support.

Chapter I

INTRODUCTION

Palaeoecological studies focus on reconstructing the environmental conditions of those living organisms we find today as fossils. Data from these fossil organisms can provide long detailed records of past climatic changes. Such records supply insight into natural climate variations over long and short periods of time and how these fluctuations, such as temperature, have affected past and present ecosystems.

Chironomid (midge) larvae are one of the most abundant aquatic organisms found in freshwater lakes. The larval phase consists of four instars. During each instar, there is a period of growth which is followed by the shedding (ecdysis) of the exoskeleton (Walker, 1987). This exoskeleton includes the head capsule, which is a heavily sclerotized structure made of chitinous material that preserves well in sediments, often for thousands of years (Hofmann, 1986). In addition, most species have specific ecological requirements and a single lake can contain over one hundred different species (Heiri, 2004). This allows for the use of chironomid head capsules as palaeoecological indicators. More specifically, researchers have used midge assemblages in lake systems to reconstruct changes in environmental variables such as salinity, lake productivity, oxygen content, acidity, lake level changes, predation pressure, catchment disturbance and, as is the focus of this study, temperature (Kurek et al., 2004).

Since chironomids have short life cycles and are capable of rapid dispersal, they respond more quickly to climate change than many other organisms, including forest vegetation (Walker, 1987). Increasing recognition of their sensitivity has allowed chironomid paleoecology to evolve from use in reconstructing pronounced late-glacial climatic changes to reconstructions of much more subtle Holocene changes, such as temperature fluctuations (Heiri, 2004).

Throughout the Holocene, the northern hemisphere has undergone several climate changes, cycles and events (Hebda, 1995). One such event is the Milankovitch thermal maximum, which occurred in the early Holocene. This period of warmth is evident at southern British Columbia sites (Walker & Pellatt, 2003); however, it does not appear to occur at the same time or be of the same intensity in the north (Kaufman et al., 2004). In this study, I use midge fossils to examine temperature change over the last 12,000 (calibrated) years at two alpine lakes in northern British Columbia, as it is an area lacking in paleoclimatic work. In particular, I test for the presence and timing of the Milankovitch thermal maximum in the region.

Chapter II

LITERATURE REVIEW

The Earth's climate is changing before our very eyes. We call this phenomenon global warming. However this is not the first time an event like this has taken place. Whether it is changes in temperature, precipitation, vegetation or atmospheric and oceanic circulation patterns, the Earth's climate has oscillated throughout time. This is why one can not simply understand recent climate change without also looking to the past. In the present study, I will use fossil chironomids to travel back to the beginning of the Holocene, just as the glaciers were retreating in the northern hemisphere.

2.1 Chironomids as Indicators of Climate Change

Chironomid larvae (Order Diptera; Family Chironomidae) live in freshwater lake sediments, wet soils, dung, streams and littoral marine environments or colonize hard submerged surfaces such as rocks, plants or wood (Heiri, 2004). Larvae are quite abundant in these communities and the larval phase comprises four stages, or instars. During each instar, there is a period of growth which is followed by the shedding (ecdysis) of the exoskeleton (Walker, 1987). This exoskeleton includes the head capsule, which is a heavily sclerotized structure made of chitinous material that preserves well in sediments (Hofmann, 1986). The rest of the larval body is quite delicate and is seldom well preserved (Walker, 1987). Chironomid larvae can range anywhere from one to thirty millimeters in length in their fourth instar (Oliver & Roussel, 1983). The larval phase is followed by a pupal phase, where there is a reorganization of the midge into the adult form. The pupa reaches the surface of the water when mature, where a winged adult emerges. The adult stage allows for the dispersal and reproduction of the chironomid (Walker, 1987), with the female typically depositing eggs into water or onto a wet surface.

Often over one hundred different species of chironomids can be found in a single lake. Most of these species have specific ecological requirements and have traditionally been used as biomonitoring organisms (Heiri, 2004). More specifically, researchers have used midge assemblages in lake systems to reconstruct changes in environmental variables such as air and surface-water temperatures, salinity, lake productivity, oxygen conditions, acidity, lake level changes, predation pressure and catchment disturbance (Kurek et al., 2004). The fossilized remains of chironomid head capsules are abundant in lake sediments and can be preserved for thousands of years. This allows for the reconstruction of past midge faunas and the types of environments in which they lived (Heiri et al., 2003).

Since chironomids have short life cycles (commonly less than one year), and are capable of rapid dispersal, it is thought that they respond more rapidly to climate changes than many other organisms, such as forest vegetation (Walker, 1987). Chironomid assemblages are affected by both direct and indirect changes in climate, sometimes making it difficult to reconstruct palaeoenvironments during relatively stable time periods, such as the Holocene (Kurek et al., 2004). However, quantitative organism-based inference models are being developed that increase the usefulness of midges in reconstructions of low magnitude changes from the Holocene, such as temperature fluctuations (Heiri, 2004).

Temperature is believed to have a direct effect on midges. For example, most Chironominae and Tanypodinae are adapted to warm conditions while most Orthocladiinae and Diamesinae appear to prefer cold conditions. Temperature is one of the major factors that controls chironomid pupation, emergence, growth, feeding and hatching of larvae. Much of their life cycle is linked to temperature. For instance, warm water temperatures during the summer can increase the rate of larval growth (Armitage et al., 1995). In addition, adults will only lay eggs if the air temperature is optimal (Larocque & Hall, 2003). Because of this, temperature variations directly influence chironomid faunal assemblages in lake systems.

Reconstructions of past summer temperatures can be produced using quantitative chironomid-temperature inference models. These models are normally based on surface-sediment samples from a number of lakes spanning a temperature gradient. Cores are taken from the deepest part of the lake basin, as this is where the highest concentration of head capsules are typically found, and head capsules are analyzed from the uppermost sediments (Heiri, 2004). For example, this was performed on a series of lakes in Labrador, Canada. The assemblages of chironomids in these lakes were found to be directly related to the surface-water temperatures in the summer. This enabled the reconstruction of former lake surface temperatures in the area (Walker et al., 1991). Similar work has also been completed in British Columbia (Barley et al., 2006; Palmer et al., 2002). Since air temperature is correlated with surface-water temperature, faunal assemblages usually also reflect air temperature changes (Larocque & Hall, 2003). Low elevation lakes fed by glacial meltwater, however, may have a cold water fauna unrepresentative of local air temperature conditions (Brooks & Birks, 2000).

2.2 The Cordilleran Ice Sheet in Northern British Columbia

The pattern of glaciation in northern British Columbia is thought to have been similar to the pattern in the southern portion of the province, apart from one major difference. Throughout the Pleistocene, ice sheet flow was controlled by topography in the south, even at the glacial maximum. To date, no evidence has been found to indicate that a single ice divide ever existed in the south that would have been capable of generating topographically-independent ice flow during the last glacial maximum (McCuaig & Roberts, 2002). Several small ice divides have been proposed in this area and evidence exists that ice flow movement was confined to valleys as it passed through the Coast Mountains (Ryder & Maynard, 1991).

Conversely, ice flow patterns in northern British Columbia did not appear to be controlled by topography during glacial maximums. Evidence from high elevation sites showing ice flow indicators in the Nass River area suggests that ice was very thick and actually submerged the mountain tops. Ice would have flowed directly over mountain peaks and across valleys during the last glacial maximum. The ice needed to maintain a minimum thickness of 1,710 meters in order to flow independent of topography. During the last glacial maximum in the Late Wisconsin, it is thought that ice streamed from an ice divide located in the Skeena Mountains south-west across the Nass River area (McCuaig & Roberts, 2002).

In the Babine Lake region, a three-phase model of ice flow has been proposed that is also applicable to the rest of northern British Columbia (Clague, 1984; Dixon-Warren & Hickin, 2000; Stumpf et al., 2000). During the ice expansion phase, ice flowed from accumulation areas in the mountains and was primarily controlled by topography. The maximum phase achieved thicknesses that allowed flow to be independent of topography. During the late glacial phase, when ice was beginning to retreat, flow was again dependant on topographic restraints (Stumpf et al., 2000).

The presence of thicker ice in the north compared to the south may have been the result of the location of storm tracks during glacial times. During the last glacial maximum, storm tracks were diverted north along the coast of the province. This enabled air masses to take up increased amounts of water from the ocean before migrating east across northern British Columbia. These factors plus the higher latitude allowed for higher amounts of precipitation, leading to thicker ice accumulation in the north. Consequently, it is believed that the continental phase of glaciation reached all of northern British Columbia (McCuaig & Roberts, 2002).

The most recent glaciation in northern British Columbia occurred during the Late Wisconsin. This event, locally termed the Fraser Glaciation, transpired in a similar fashion to the southern portion of the province. During the early phase, ice spread outwards from accumulation centers in the Coast, Cassiar and Skeena Mountains. However, unlike in the south, ice also grew and formed in the interior plateau, such as was seen in the Stikine. Regional reversals in ice flow directions also arose due to changes in volume of ice surging from mountains relative to outflow from an intermontane ice dome. Local shifts in ice flow directions also occurred due to the forcing of topography on thickening ice (Ryder & Maynard, 1991).

The presence of Glacial Lake Stikine in the Stikine valley during the early Fraser suggests that there was a long mountain glaciation phase before an ice sheet was completely formed (Ryder & Maynard, 1991). The lake was created through the damming of the Stikine River by glaciers flowing from the Coast Mountains (Spooner & Osborn, 2000). Thick glaciolacustrine sediments mark the area that the glacial lake once occupied. Several other glacial lakes were formed in the early phase in river valleys crossing the Coast Mountains as well as in eastward draining valleys (Ryder & Maynard, 1991).

During the height of the Fraser Glaciation the Coast Mountains did not appear to support a continuous ice divide nor did ice from here move eastward. However, there is evidence that some outlet glaciers drained west through these mountains towards the Pacific Ocean. The northern Skeena Mountains, which supported an ice dome, dominated much of the eastern lowlands below the Coast Mountains with radial ice flow. Ice also flowed from the northern Cassiar Mountains south-west to join the Teslin ice stream and north-east to the Liard ice stream.

A broad ice stream moved north to the southern portion of the Cassiar Mountains then turned eastwards and flowed across the Liard Lowlands on its way to the margin of the ice sheet. Another major ice stream migrated north-west to the Teslin Depression and into the Yukon. Other ice streams that also existed included one that flowed north-west of Finlay to the Liard Lowland, one that flowed south through the Nass Depression, Takla and Babine Lake valleys and one that flowed from south of Finlay River east to merge with ice tracking south in the Rocky Mountain Trench (Ryder & Maynard, 1991). Several glacial lakes were formed in valleys through damming by advancing glaciers, however drainage in eastern valleys remained open (Plouffe & Levson, 2001).

During deglaciation, ice lobes and valley glaciers underwent frontal retreat while stagnant ice was downwasted. As ice thinned, glaciers were confined to fiords and valleys and topographic control was increased causing changes in ice flow directions (McCuaig & Roberts, 2002). In addition, ice lobes and ice streams did not all recede at the same time (Ryder & Maynard, 1991). For example, the Atlin area bears evidence that there were several offset and locally competing ice lobes (Tallman, 1975). Some ice may have been thermally stratified, with colder ice over the warm, causing the formation of several subglacial meltwater channels. One such channel was involved in the formation of the postglacial Grand Canyon of the Stikine. Several were also located through the Nass Depression and in parts of the Iskut River valley (Ryder & Maynard, 1991). Ice marginal drainage networks were also present throughout the extent of the receding ice sheet (Spooner & Osborn, 2000).

Throughout the intermontane plateaus, and Omineca and Cassiar Mountains, meltwater channels were abundant. Positions of these channels can help researchers determine where the ice margins were once located. All through valley floors and lowlands lay extensive glaciofluvial features such as eskers, kames, delta kames and outwash terraces. Meltwater channels which contain eskers are abundant in the central Stikine plateau. Some of these eskers are formed obliquely across the channels which could indicate that the channels were originally tunnel valleys and after partial closure occurred, eskers formed. Extensive erosion caused by the catastrophic draining of an ice-dammed lake caused a scabland to form near the village of Tahltan (Spooner & Osborn, 2000). The absence of a retreat-phase glacial lake in the Stikine River valley indicates that the Stikine glacier occupied the area until deglaciation. It began to recede as meltwater from the surrounding ice sheet moved subglacially. In the Nechako River valley and Knewstubb Lake region glacial lakes were impounded by glacial withdraw (Plouffe & Levson, 2001). Increased sea level as well as thinning ice caused glaciers from the coast to shrink back through the Coast Mountains (Ryder & Maynard, 1991).

Glacial resurgences and standstills are evident from the presence of recessional moraines. These indicate former ice sheet margins and are absent in southern British Columbia. Areas supporting such features include the Tuya-Teslin area, the valleys in Level Mountain range and valleys in the Omineca Mountains (Ryder & Maynard, 1991). In general, most valleys were ice-free by 12,000-10,500 ^{14}C yr BP (Dyke, 2006).

2.3 <u>Holocene Climatic Events</u>

Over the last 12,000 (calibrated) years, the northern hemisphere has undergone several climate changes, cycles and events. Prominent climatic events include the Milankovitch thermal maximum, the Preboreal Oscillation, the 8,200 cal. yr BP cooling event and the Little Ice Age.

2.3.1 <u>Milankovitch Thermal Maximum</u>

The Milankovitch theory of the ice ages proposes that variations in the Earth's orbital parameters and the resulting redistribution of insolation across the surface of the Earth had a major part in controlling glaciation in the past (Bradley, 1999). Milankovitch (1941) took Pilgrim's (1904) orbital calculations and applied them to the laws of radiation. From this, he constructed a set of curves for summer and winter half-years that explained how irradiation intensity varied as a function of time and latitude over the past 600,000 years. He found that variations in the amount of insolation received at 65ºN during the summer half-year were greater than 8% of modern values. He concluded that the amount of summer insolation received at northern latitudes had a key role in controlling the expansion and contraction of the ice sheets. This has come to be known as the Milankovitch theory.

The orbital parameters that cause changes in solar insolation include the eccentricity of Earth's orbit, the obliquity of tilt of Earth's axis and the precession of Earth's axis of rotation. Changes in any of these elements that cause a shift in received irradiation will undoubtedly cause a certain degree of climate change (Imbrie & Imbrie, 1980). These cycles may produce variations of up to 10ºC in air temperature (Harris, 2002). Milankovitch cycles can account for long-term changes in climate spanning thousands of years. However, short-term changes (less than 1000 years) in insolation are also evident, arising from other effects, including changes in solar activity. For example, over the last 140 years, approximately half of the variation in northern hemisphere air temperatures can be accounted for by changes in solar activity (Walker & Pellatt, 2003). Before 1850, almost half of the variation in air temperatures on a decadal scale can be explained by a combination of solar variability and volcanism (Crowley, 2000).

Eccentricity, which varies over time, is a measure describing how circular or elliptical an orbit is. If there is low eccentricity the Earth's orbit is more circular and the Earth is the same distance from the sun during all seasons, meaning there are no seasonal differences in total insolation. If there is high eccentricity, the orbit is more elliptical and the Earth is more distant from the sun during some seasons, meaning there are seasonal differences in the total insolation received by the Earth. This parameter has two overlapping cycles, at 100,000 and 413,000 years. Currently, the Earth's orbit is slightly elliptical.

The tilt of the Earth's axis varies from 21.8º to 24.4º and has a 41,000 year cycle. The tilt generates the seasons and is most pronounced at high latitudes. If there were no tilt there would be no distinct seasons. A large tilt would generate large differences between the summer and winter seasons. Currently, the Earth has a 23.4º tilt to its axis and this is decreasing (Berger & Loutre, 1991).

The precession determines the season when the Earth is closest to the sun. At present, the Earth is closest to the sun on January 3 (perihelion) and is farthest on July 5 (aphelion). The Earth receives 3.5% more radiation at the perihelion. This effect is most pronounced at low latitudes and has two overlapping cycles, at 19,000 and 23,000 years. If the Earth were to have low eccentricity, the precession effect would be small, whereas a high eccentricity would cause a greater precession effect (Bradley, 1999).

The Milankovitch thermal maximum (MTM) refers to a warm interval coincident with the peak of Holocene summer solar insolation. Summer solar insolation at high northern latitudes climaxed during the first half of the Holocene and several researchers have suggested that summer thermal conditions were on the order of 10% warmer than present (Ritchie, 1985; Kaufman et al., 2004). However, this warming does not appear to occur at the same time or be of the same intensity at all locations (Kaufman et al., 2004).

During the early Holocene, evidence of warmer temperatures appears to be concentrated in northwestern North America. Cooler conditions likely remained in the north-east and have been attributed to the lingering Laurentide Ice Sheet. In general, dates for the MTM in Alaska and northwestern Canada range between 11,000 and 9,000 ^{14}C yr BP (13,000 and 10,200 cal. yr BP). This is approximately 4,000 years prior to the interval of maximum warmth in northeastern Canada. One study at Cabin Lake in the Cascade Mountains of southern British Columbia dated the MTM at 10,000 to 7,000 ^{14}C yr BP (11,400 to 7,700 cal. yr BP), yet at nearby 3M Pond, it appeared to occur from 10,000 to 4,000 ^{14}C yr BP (11,400 to 4,500 cal. yr BP) (Walker & Cwynar, 2006). In southern British Columbia at Frozen Lake, maximum Holocene temperatures were evident at 9,000 ^{14}C yr BP (10,200 cal. yr BP) (Rosenberg et al., 2004). Such studies clearly show the discrepancies that occur in dating of this climatic event. Finally, recent midge analysis in Yukon and Alaska suggests that the MTM was not as strong as it was in southern British Columbia (Barley, 2004; Stepanovic, 2006).

2.3.2 Preboreal Oscillation

The Preboreal Oscillation (PBO) was a short-lived cooling event, approximately 150 to 250 years in length, which occurred in the early Holocene (Fisher et al., 2002). Specifically, proposed dates for the event in North America range from 9,650 to 9,600 ^{14}C yr BP (10,700 to 10,600 cal. yr BP) (Yu, 2000; Yu & Wright Jr., 2001; Cwynar et al., 2003). It has been interpreted as an effect of an increase in meltwater in the oceans. The source of the freshwater remains uncertain, however a recent study by Fisher et al. (2002) brings new evidence to light that may help to explain this phenomenon.

Lake Agassiz was the largest lake in North America during the last deglaciation (Teller et al., 2002). At 11,335 cal. yr BP (10,000 ^{14}C yr BP), as the Laurentide Ice Sheet retreated, a massive meltwater discharge event occurred resulting from the sudden drainage of the glacial lake via the Mackenzie River into the Arctic Ocean (Fisher & Smith, 1994). Episodic flows continued until about 10,750 cal. yr BP (9,700 ^{14}C yr BP), when the southern portion of Lake

Agassiz reopened and re-routed freshwater drainage into the Mississippi River system. This flood water caused a 0.062 meter rise in global sea levels. In the Beaufort region, 2-4% of the freshwater formed sea ice. The thicker long-lasting pack ice may have been washed through Fram Strait. The increased pack ice along with the enhancement of freshwater at the surface probably caused an increase in albedo and lowered ocean salinity in the area. North Atlantic Deep Water formation most likely decreased, causing a reduction in thermohaline circulation. Often referred to as the ocean conveyor belt, thermohaline circulation is the result of global density gradients caused by surface heat and freshwater fluxes, and has a large impact on the Earth's climate. This alteration in ocean circulation may have been the climate forcing mechanism responsible for the PBO (Fisher et al., 2002). An instantaneous and distinct rise in the atmospheric $^{14}C/^{12}C$ ratio confirms that the PBO was initiated by increased freshwater input into the oceans, slowing the thermohaline circulation. This may have temporarily forced the Polar Front farther south (Bjorck et al., 1997).

The PBO was first recorded in northwestern Europe. Ice cores from Greenland, showing a $\delta^{18}O$ minimum during the oscillation (Wagner et al., 1999), and several North American terrestrial and marine records, document this event (Johnson et al., 1992; O'Brian et al., 1995; Bjorck et al., 1996, 1997; Hald & Hagen, 1998; Yu, 2000; Yu & Wright Jr., 2001; Cwynar et al., 2003). Records from Greenland suggest that, due to the cooler climate and increased precipitation, the PBO was typified by ice readvances. It was not until the end of the oscillation, when the climate began to warm, that land-based ice sheets began to melt again (Bjorck et al., 1997). It has been suggested that the climatic oscillation was widespread and likely occurred over the entire northern hemisphere rather than as a local meltwater-induced climate cooling (Yu & Wright Jr., 2001).

2.3.3 <u>8,200 cal. yr BP Cooling Event</u>

The 8,200 cal. yr BP (7,500 ^{14}C yr BP) cooling event lasted for 200 years and was the most extreme cold episode to occur after the Younger Dryas (11,000 to 10,000 ^{14}C yr BP or 13,000 to 11,400 cal. yr BP). The 8,200 cal. yr BP cooling event was first documented in Greenland ice cores using oxygen-isotope analysis (Hammarlund et al., 2005). A record low in $\delta^{18}O$ occurred at approximately 8,200 cal. yr BP in the cores, indicating a cooler climate (Klitgaard-Kristensen et al., 1998). Temperature estimates based on this analysis suggest that the climate over Greenland cooled about 6±2ºC between 8,400 and 8,000 cal. yr BP (7,800 and 7,300 ^{14}C yr BP) (Alley et al., 1997). Other climate records, including marine documentation from the northern North Sea and tree-ring data from Germany, propose a temperature drop of 2ºC over the North Atlantic region around this time (Klitgaard-Kristensen et al., 1998). Evidence from North America, such as pollen records from the east (Shuman et al., 2002), lake sediment records from the White Mountains in the east (Kurek et al., 2004) and from Crawford Lake in Ontario (Yu & Eicher, 1998), a fossil stomata record from BC2 Lake in northeastern British Columbia (Pisaric et al., 2003) and ice core records from the Canadian high-Arctic (van Grafenstein et al., 1998), suggests that the cold period also occurred in the western half of the northern hemisphere.

Hypotheses concerning the cause of this cold period also center on a major outburst of meltwater from Lakes Agassiz and Ojibway. The outburst coincided with the final collapse and retreat of the Laurentide Ice Sheet near Hudson Bay and has been dated at 7,700 ^{14}C yr BP (8,300 cal. yr BP), just prior to the cooling. The volume of freshwater released by the glacial lakes has been estimated at 163,000 km^3 (Teller et al., 2002). The pulse of freshwater discharged through Hudson Bay and Hudson Strait into the Labrador Sea, freshening the North Atlantic surface waters (Dean et al., 2002). Thermohaline circulation was again interrupted by suppression of the North Atlantic Deep Water formation (Teller et al., 2002), which led to an increase in sea-ice cover in the North Atlantic and reduced the moist and mild Atlantic air that penetrated the surrounding land masses. The results included drought conditions in Greenland (Alley et al., 1997) and a southerly displacement of the polar front (Bond et al., 2001), leading to a southerly displacement of storm tracks over the North Atlantic, resulting in subsequent cooling (Magny et al., 2003).

2.3.4 Little Ice Age

The Little Ice Age (LIA) was the most recent glacier expansion event of the late Holocene. This cooling episode followed the Medieval Climate Optimum, a warmer era that occurred throughout Europe from the tenth to the fourteenth century. The LIA is thought to have begun in the thirteenth or fourteenth century and lasted until the mid-nineteenth century (Reyes et al., 2006). Although it occurred on a global scale, the underlying causes and regional differences in timing of the event are still under debate (Grove, 2001).

Climate during this time appeared to vary on small scales, both spatially and temporally. In the Canadian Rocky Mountains, glacier advances began in the twelfth and thirteenth centuries (Grove, 2001). This is apparent from detailed evidence obtained at the forefield of the Robson Glacier. Within abandoned stream channels inside the terminal moraine, detrital logs and *in situ* tree stumps show evidence of having been shaved and killed by ice, later to be exposed and dated. Ring-width and maximum-density chronologies were developed from these and were cross-dated with long tree chronologies to indicate that ice began to advance into the forest between AD 1142 and 1150 and continued to do so until approximately AD 1350 (Luckman, 1995).

In northwestern North America there is some evidence of synchronicity in the timing of the LIA, as is suggested from well-dated glacier records using tree rings from the Canadian Rocky Mountains (Luckman, 2000), coastal Alaska (Calkin et al., 2001) and the southern Coast Mountains of British Columbia (Smith & Desloges, 2000; Larocque & Smith, 2003; Lewis & Smith, 2004). In these areas, glacial advances became more extensive over the last 3,000 years, building up to a maximum in the eighteenth and nineteenth centuries (Luckman, 1994). Luckman attributed this glacial activity to the long-term decrease in received solar radiation due to fluctuations in the Earth's orbit (i.e., Milankovitch cycles). Decreased sunspot activity has also been suggested as a reason for decreased solar output. During the period of 1645-1715, sunspot activity was at its lowest (Maunder Minimum), and this happens to fall right in the middle of the cooling period. The other theory as to the cause of glacial advance and the LIA is an increase in volcanic activity. When massive eruptions occur, ash can reach high into the atmosphere and can spread great distances. The resulting ash cloud can block out insolation, leading to a cooling in the affected areas. Sulfur, in the form of sulfur dioxide gas, is also released into the atmosphere. Once it reaches the stratosphere it turns into sulphuric acid particles and further decreases the solar radiation reaching the Earth by reflecting the sun's rays. It is difficult to differentiate the effects that decreased solar output and increased volcanic activity had on the glacial advances during the past 1,000 years because they occur at the same time. However, between AD 1520 and 1650, they are uncorrelated and a magnetic susceptibility record provides evidence that it was a decrease in solar radiation (decreased sunspot activity) reaching the Earth that caused variations in glacier advances and retreats during the LIA (Polissar et al., 2006).

2.4 Palaeoclimate of Northern British Columbia

The palaeoclimatic record for northwestern British Columbia has been based mainly on studies utilizing fossil pollen and geomorphic evidence (Figure 2.1 & Table 2.1). To date, only two studies, at Susie and Pyramid Lakes (Spooner et al., 1997; Mazzucchi et al., 2003), have been conducted in the western interior mountains of the northwestern Cordillera, which is where the present study was carried out.

The Holocene record at Susie Lake was studied by Spooner et al. (1997) using pollen, macrofossil and sedimentological evidence. Shrub and herb assemblages were present from 10,200-8,400 cal. yr BP, but were quickly replaced by spruce (*Picea*) and subalpine fir (*Abies lasiocarpa*) forests (8,400-4,500 cal. yr BP) as warmer-than-present climatic conditions dominated the area. Treeline increased in elevation from 6,000-1,900 cal. yr BP. The migration of *Pinus contorta* into the region was indicated by the increase in pine pollen in the record (5,800-4,500 cal. yr BP). Spruce (4,500 cal. yr BP) and fir (1,900 cal. yr BP) needles disappeared from the record, pointing to a decreased treeline, likely below the elevation of the lake, and the establishment of the modern cold and moist climate. Western hemlock (*Tsuga heterophylla*) pollen increased at 1,900 cal. yr BP, around the same time that a change in air mass circulation patterns occurred, increasing storm frequency in the area.

Holocene climate changes at Pyramid Lake were studied by Mazzucchi et al. (2003) using pollen, plant macrofossils, charcoal and clastic sediments. Since deglaciation at 12,800 cal. yr BP, several high-magnitude rainstorm events and timberline migration occurred. White spruce (*Picea* cf. *glauca*) was present near the lake during four of these rainstorm events (5,900-5,000 cal. yr BP), however a closed forest-stand did not develop at the lake at any point during the Holocene. Since 10,500 cal. yr BP, subalpine fir (*Abies lasiocarpa*) was present above the

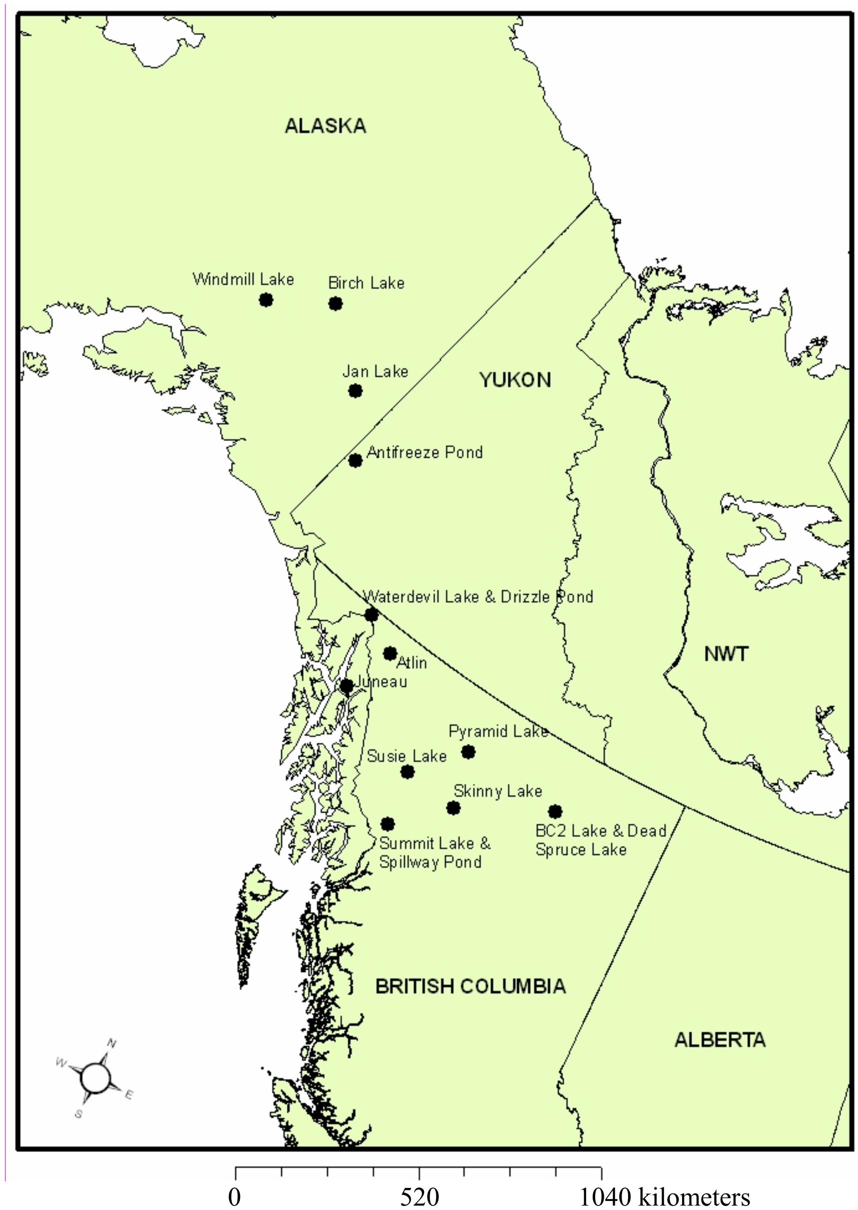

Figure 2.1: Map showing palaeoenvironmental study sites in northern British Columbia and surrounding areas. Windmill, Birch and Jan Lake were studied by Stepanovic (2006) using midges, Antifreeze Pond was studied by Barley (2004) using midges, Waterdevil Lake and Drizzle Pond were studied by Spear and Cwynar (1997) using the fossil record, a transect from Juneau to Atlin was studied by Miller and Anderson (1974) using Quaternary glacial sequences and palynological profiles in kettle-hole bogs, Susie Lake was studied by Spooner et al. (1997) using pollen, macrofossil and sedimentological records, Summit Lake and Spillway Pond were studied by Clague and Mathewes (1996) using geomorphic, stratigraphic and palaeoecological evidence, Pyramid Lake was studied by Mazzucchi et al. (2003) using pollen, plant macrofossils, charcoal and clastic sediments, Skinny Lake was studied by Spooner et al. (2002) using lithostratigraphic and biotic proxies and BC2 Lake and Dead Spruce Lake were studied by Pisaric et al. (2003) using fossil pollen and stomata. The results of these studies are summarized in Table 2.1.

Table 2.1: A comparison of palaeoclimatic reconstructions performed in northern British Columbia and surrounding areas. The study sites are organized on a west to east gradient, with Windmill Lake, Alaska located the farthest west and BC2 Lake, British Columbia located the farthest east.

<table>
<tr><th>Calendar Years (cal. yr BP)</th><th>Windmill Lake (AK)</th><th>Birch Lake (AK)</th><th>Jan Lake (AK)</th><th>Antifreeze Pond (YK)</th><th>Drizzle Pond (BC)</th><th>Waterdevil Lake (BC)</th><th>Juneau-Atlin Transect (AK-BC)</th></tr>
<tr><td>0</td><td rowspan="15">Modern temperatures</td><td rowspan="17">Modern temperatures</td><td rowspan="20">Modern temperatures</td><td rowspan="19">Modern temperatures</td><td rowspan="3">Neoglaciation & increased precipitation (due to changes in air mass circulation)</td><td rowspan="8">Cool & wet</td><td rowspan="2">Warm & wet</td></tr>
<tr><td>500</td></tr>
<tr><td>1,000</td><td rowspan="4">Cool & dry with decreased storminess</td></tr>
<tr><td>1,500</td><td rowspan="26"></td></tr>
<tr><td>2,000</td></tr>
<tr><td>2,500</td></tr>
<tr><td>3,000</td><td rowspan="2">Warm & wet</td></tr>
<tr><td>3,500</td></tr>
<tr><td>4,000</td><td rowspan="21"></td><td rowspan="5">Warm & wet with increased storminess</td></tr>
<tr><td>4,500</td></tr>
<tr><td>5,000</td></tr>
<tr><td>5,500</td></tr>
<tr><td>6,000</td></tr>
<tr><td>6,500</td><td rowspan="4">Warm & wet</td></tr>
<tr><td>7,000</td></tr>
<tr><td>7,500</td><td rowspan="2">Cool</td></tr>
<tr><td>8,000</td></tr>
<tr><td>8,500</td><td rowspan="3"></td><td rowspan="3">Cool</td><td rowspan="9">Cool & dry</td></tr>
<tr><td>9,000</td></tr>
<tr><td>9,500</td><td rowspan="7">Cool</td></tr>
<tr><td>10,000</td><td rowspan="2">Warm</td><td rowspan="2"></td><td rowspan="4">Warm</td></tr>
<tr><td>10,500</td></tr>
<tr><td>11,000</td><td></td><td>Warm</td></tr>
<tr><td>11,500</td><td rowspan="3">Cool</td><td rowspan="3">Cool</td></tr>
<tr><td>12,000</td><td rowspan="5"></td></tr>
<tr><td>12,500</td></tr>
<tr><td>13,000</td><td rowspan="3"></td><td rowspan="3"></td><td rowspan="3">Modern temperatures</td><td rowspan="3"></td></tr>
<tr><td>13,500</td></tr>
<tr><td>14,000</td></tr>
</table>

Table 2.1: Continued from previous page.

<table>
<tr><th>Calendar Years (cal. yr BP)</th><th>Susie Lake (BC)</th><th>Summit Lake & Spillway Pond (BC)</th><th>Pyramid Lake (BC)</th><th>Skinny Lake (BC)</th><th>Dead Spruce Lake (BC)</th><th>BC2 Lake (BC)</th></tr>
<tr><td>0</td><td rowspan="4"></td><td>Warm & dry</td><td rowspan="3">Change in air mass circulation</td><td rowspan="7">Cool & wet with changes in air mass circulation</td><td rowspan="16"></td><td rowspan="5"></td></tr>
<tr><td>500</td><td>Cool & wet</td></tr>
<tr><td>1,000</td><td rowspan="2"></td></tr>
<tr><td>1,500</td><td rowspan="4">Increased precipitation</td></tr>
<tr><td>2,000</td><td rowspan="4">Modern climate with increased storminess (due to changes in air mass circulation)</td><td rowspan="2">Neoglaciation</td></tr>
<tr><td>2,500</td><td rowspan="2">Warm</td></tr>
<tr><td>3,000</td><td rowspan="23"></td></tr>
<tr><td>3,500</td><td rowspan="2"></td><td rowspan="6">Modern climate</td><td rowspan="9"></td></tr>
<tr><td>4,000</td><td rowspan="8">Warmer than present</td></tr>
<tr><td>4,500</td><td rowspan="3">Warmer than present & increased storminess</td></tr>
<tr><td>5,000</td></tr>
<tr><td>5,500</td></tr>
<tr><td>6,000</td><td></td></tr>
<tr><td>6,500</td><td rowspan="3">Drier than present</td><td rowspan="2">Warmer than present</td></tr>
<tr><td>7,000</td></tr>
<tr><td>7,500</td><td rowspan="4">Cool & wet</td></tr>
<tr><td>8,000</td><td rowspan="13"></td><td rowspan="9"></td><td rowspan="2">Dry</td><td rowspan="2">Rapid cooling</td></tr>
<tr><td>8,500</td></tr>
<tr><td>9,000</td><td rowspan="11"></td><td rowspan="3">Warmer than present</td></tr>
<tr><td>9,500</td><td rowspan="2">Warm & dry</td></tr>
<tr><td>10,000</td></tr>
<tr><td>10,500</td><td rowspan="6">Cool & wet</td><td rowspan="8"></td></tr>
<tr><td>11,000</td></tr>
<tr><td>11,500</td></tr>
<tr><td>12,000</td></tr>
<tr><td>12,500</td><td rowspan="2">Deglaciation</td></tr>
<tr><td>13,000</td></tr>
<tr><td>13,500</td><td rowspan="2"></td><td rowspan="2">Deglaciation</td></tr>
<tr><td>14,000</td></tr>
</table>

elevation of the lake. Similar to Susie Lake, western hemlock (*Tsuga heterophylla*) pollen appeared at 1,300 cal. yr BP, likely due to the change in Late Holocene air mass circulation patterns.

The climate of northwestern British Columbia is governed by incursions of moist Pacific air into dry stable Arctic air masses (Mazzucchi et al., 2003). However, there are inconsistencies in the timing of palaeoclimatic change between maritime and continental interior sites. The sites in the interior mountains have a more continental climate and may yield a different record than the maritime sites strongly influenced by Pacific air (Spooner et al., 2003). For example, several studies (Cwynar, 1993; Spooner et al, 1997, 2002; Mazzucchi, 2000) have indicated that western hemlock (*Tsuga heterophylla*) pollen increased at eastern sites much later than in western sites, and long after the shift to a modern climate. They proposed that changes in Late Holocene air mass circulation initiated the dispersal of coastal pollen towards the eastern portions of the province. However, regional atmospheric circulation patterns do not appear to have changed during the Late Holocene in the south (Banner et al, 1983; Gottesfeld et al., 1991) or on the eastern borders of the province (White & Mathewes, 1982; MacDonald, 1984, 1987; MacDonald & Cwynar, 1985).

2.4.1 <u>The Late Glacial and Early Holocene</u>

According to Spooner et al. (2002) and Mazzucchi et al. (2003), northern British Columbia underwent deglaciation between 14,500-12,800 cal. yr BP. The principal vegetation at this time consisted of shrub and herb tundra, including alder (*Alnus*) and birch (*Betula*) (Stuart et al., 1989; Spear and Cwynar, 1997; Spooner et al., 1997; Pisaric et al., 2003). Cooler temperatures persisted at most sites in Table 2.1 immediately following the retreating glaciers (Miller and Anderson, 1974; Spooner et al., 2002; Barley, 2004; Stepanovic, 2006), however a regional warming occurred at several lakes between 12,000-9,000 cal yr BP (Spooner et al., 2002; Pisaric et al., 2003; Stepanovic, 2006). A short cooling interval, centered around 8,200 cal. yr BP, is observed at Skinny, Windmill and Birch Lakes (Spooner et al., 2002; Stepanovic, 2006).

2.4.2 The Middle Holocene

Vegetation in northern British Columbia transitioned from shrub and herb tundra to forests, increasing in density, during the middle Holocene (Stuart et al., 1989; Spear & Cwynar, 1997; Spooner et al., 1997; Spooner et al., 2002; Mazzucchi et al., 2003; Pisaric et al., 2003). An overall cooling trend is recorded at both Skinny and Jan Lakes (Spooner et al., 2002; Stepanovic, 2006), whereas periods of warm temperatures, with increased storminess, occurred at several other lakes in Table 2.1 (Miller & Anderson, 1974; Spooner et al., 1997; Mazzucchi et al., 2003; Pisaric et al., 2003).

2.4.3 The Late Holocene

During the late Holocene there appears to have been a significant change in regional air-mass circulation patterns in northern British Columbia. This was evident at several of the sites in Table 2.1, where a low pressure system may have caused moist Pacific air to penetrate inland resulting in higher storm frequencies with increased precipitation and cooler temperatures (Miller & Anderson, 1974; Clague & Mathewes, 1996; Spear & Cwynar, 1997; Spooner et al., 1997; Spooner et al., 2002; Mazzucchi et al., 2003). The modified air circulation patterns also initiated the dispersal of coastal pollen towards the eastern portions of the province, causing changes in vegetation (Spear & Cwynar, 1997; Spooner et al., 2002; Mazzucchi et al., 2003). However, such changes did not appear to affect the climate at Windmill, Birch and Jan Lakes in

Alaska and Antifreeze Pond in Yukon, where modern temperatures prevailed throughout this period (Barley, 2004; Stepanovic, 2006).

While these studies provide some insights into the late-glacial and Holocene palaeoclimate of northern British Columbia, the results from the research not involving midges are largely based on qualitative inferences. Through my research I intend to contribute to the palaeoclimatic record for northern British Columbia by attempting to resolve some of the inconsistencies in the timing of climate change in the continental interior, and by providing quantitative estimates of postglacial changes in temperature. More specifically, I test for the presence and timing of early Holocene warmth – the Milankovitch thermal maximum.

Chapter III

STUDY AREAS

3.1 Pyramid Lake

Pyramid Lake (58º53'N, 129º50'W) is a subalpine tarn located in the Cassiar Mountains of the northwestern Cordillera in northern British Columbia (Figures 3.1 & 3.2). It is a cold polymictic lake, partially due to the strong winds that frequent the area, and has minimal sediment mixing as a result of slumping and bioturbation. The lake is at an elevation of 1,450 meters (50 meters above treeline) and has a maximum fetch of 480 meters and a maximum depth of 9 meters. At the southern end of the lake water enters via a groundwater stream. Water exits the basin over and through volcanic and metamorphic bedrock. The average annual precipitation for the area is 700 mm, with 60% as snow, and the mean annual air temperature is -3.2ºC. The daily average July temperature (1971-2000) recorded at the Dease Lake climate station, located at an elevation of 806.6 meters, is 12.8°C (Environment Canada, 2008). Assuming a lapse rate of 6°C/1000 meters, the corrected daily average temperature for July (1971-2000) at Pyramid Lake is 8.9ºC. Abrupt and violent convective showers frequent the region during the summer. The area experiences discontinuous permafrost and is located within the transition between spruce-willow-birch and alpine tundra biogeoclimatic zones. Immediately surrounding Pyramid Lake is an alpine tundra consisting of grass, sedge, shrubs of alder (*Alnus sinuata*), willow (*Salix arctica* and *Salix planifolia*), dwarf birch (*Betula glandulosa*) and krummholz subalpine fir (*Abies lasiocarpa*). The slopes and ridges above the lake are sparsely vegetated and consist of patches of deciduous shrubs, grasses and sedges. The eastern slope contains three vegetated gullies while the western

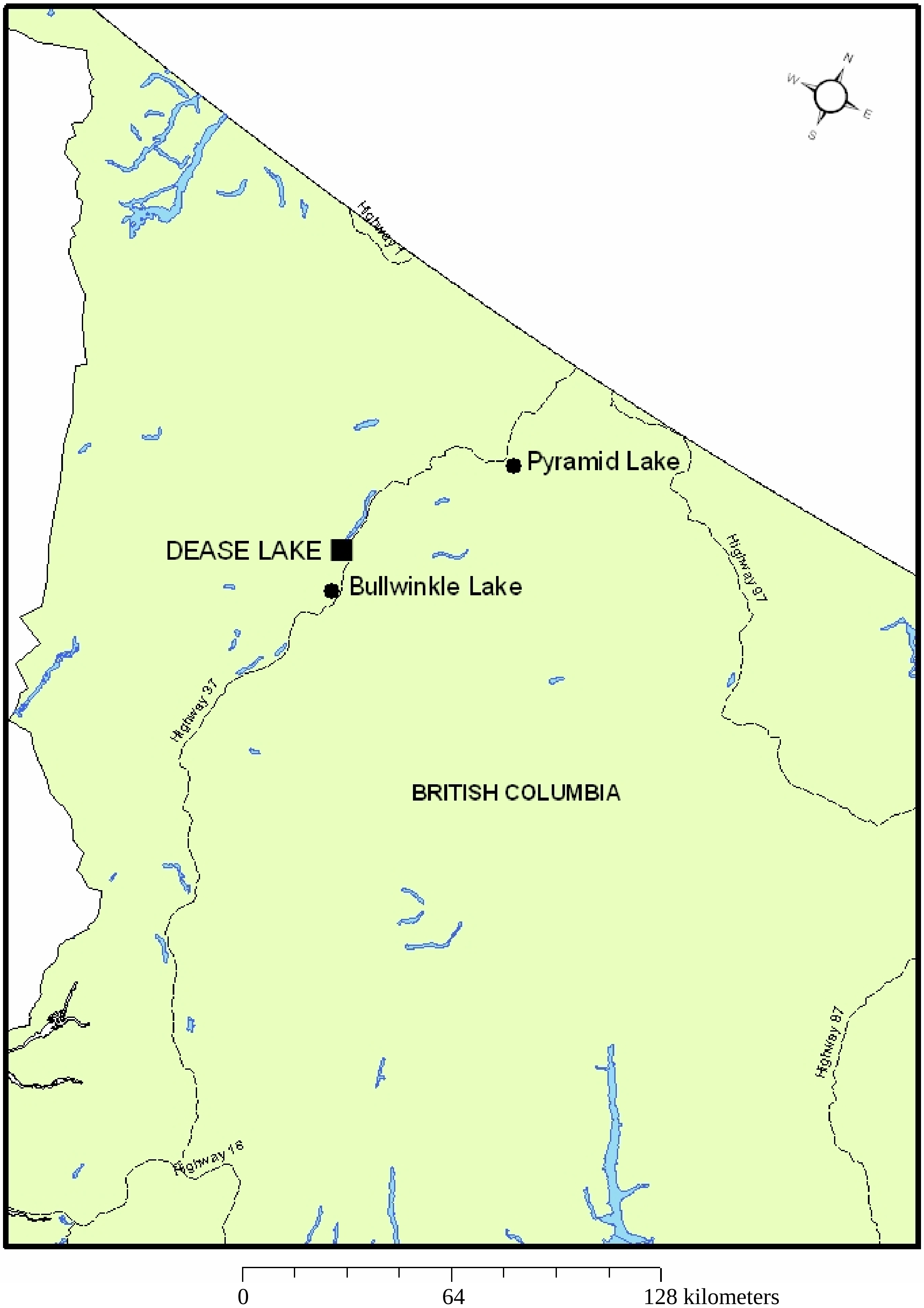

Figure 3.1: Map indicating location of Pyramid and Bullwinkle Lakes, in the Cassiar Mountains of the northwestern Cordillera in northern British Columbia.

Figure 3.2: Photograph of the northward view across Pyramid Lake (courtesy of David Mazzucchi).

slope consists of a steep talus (Mazzucchi et al., 2003). This particular lake was selected for this study because previous work had been conducted on it by Mazzucchi et al. in 2003 and they had material available for further studies.

3.2 Bullwinkle Lake

Bullwinkle Lake (58º15'N, 129º52'W) is an alpine pond located in the Cassiar Mountains of the northwestern Cordillera in northern British Columbia (Figures 3.1 & 3.3). It is a polymictic lake, due to its position in a wind corridor. This might cause currents that result in some sediment resuspension. The lake is at an elevation of 1,313 meters (200 meters below treeline) and has a maximum depth of less than 2 meters. It is possibly fed by a groundwater inlet as well as snowmelt streams. There is a surface-water outlet located at the southeast end of the lake, although it has been dammed by beaver activity. It appears that the basin was not formed by beavers, although the surface level of the lake may have been raised by about 1 m throughout the Holocene. Beavers do not appear to be currently active at the lake. Bullwinkle Lake is located in the forest-tundra transition zone, and immediately surrounding the lake is white spruce (*Picea glauca*), subalpine fir (*Abies lasiocarpa*), lodgepole pine (*Pinus contorta*), dwarf birch (*Betula glandulosa*) and willow (*Salix arctica* and *Salix planifolia*). The daily average July temperature (1971-2000) recorded at the Dease Lake climate station, located at an elevation of 806.6 meters, is 12.8°C (Environment Canada, 2008). Assuming a lapse rate of 6°C/1000 meters, the corrected daily average temperature for July (1971-2000) at Bullwinkle Lake is 9.8ºC. This particular lake was selected for this study due to its accessible location, ideal size and shallow depth.

Figure 3.3: Photograph of the northward view across Bullwinkle Lake. Shown in the foreground is a section of the lake flooded by beaver activity.

Chapter IV

METHODS

4.1 Core Collection and Lithology

Palaeoclimatic work had already been completed on Pyramid Lake by Mazzucchi et al. in 2003. They obtained the PYR3 core from Pyramid Lake using a modified percussion corer (Gilbert & Glew, 1985; Reasoner, 1993). The core was x-rayed using a Pickard Industrial x-ray unit to determine stratigraphy. Sub-sampling occurred approximately every 5 cm, and from each interval 1 cm^3 samples were removed and were analyzed for pollen, magnetic susceptibility (Sapphire Instruments-2B™), dry bulk density and loss on ignition (LOI 550ºC and LOI 950ºC after Dean, 1974). Microscopic charcoal analysis (Waddington, 1969) was also performed on each interval with 2 cm^3 samples. A combined needle record was also created using correlations of macrofossil depths in PYR1, PYR2 and PYR3. No chironomid work was performed by Mazzucchi et al. (2003).

A Kajak-Brinkhurst corer (Glew, 1989) was used to obtain the uppermost sediments from Bullwinkle Lake at a water depth of 1.6 m. This core was sub-sampled every 1 cm and had a total length of 35 cm. A Livingstone piston corer (Wright, 1967) was used to remove three cores (BULL1, BULL2 and BULL3) from Bullwinkle Lake on August 25, 2006. These were taken from the deepest part of the lake, with a measured depth of 1.55 m. The extracted cores penetrated to a sediment depth of 1.70 m. The surface water temperature, conductivity, pH and dissolved oxygen were recorded at depths of 0 and 1 m in Bullwinkle Lake as measured with a Hydrolab. All cores were transported to UBC-Okanagan where they were stored in a cold room at 4ºC.

4.2 Chronology

Mazzucchi et al. (2003) obtained four samples for AMS radiocarbon dating from Pyramid Lake. Eight samples were obtained for AMS radiocarbon dating from Bullwinkle Lake. Samples were sent to Paleotec Services in Ontario for analysis. Dates from both Pyramid and Bullwinkle Lakes were calibrated using CALIB REV5.0.2 (Stuiver & Reimer, 1986-2008).

4.3 Midge Analysis

Processing of each sub-sample from both lakes followed the procedures outlined by Walker et al. (1991) and Walker (1987, 2001). Midge analysis was performed on the PYR3 core from Pyramid Lake and the BULL1 and BULL2 cores from Bullwinkle Lake. The amount of sediment used from each sub-sample ranged from 0.5 to 2 cm^3, depending on the number of chironomids present. A minimum of 50 chironomid head capsules are needed from each interval for statistical purposes. To remove any carbonates from the sediments, each sample was treated with 10% HCl. To complete the deflocculation, 5% KOH was added to the samples and heated to 45-60ºC for 2-5 minutes. Sediments were rinsed on a 100 micrometer mesh sieve and the residue transferred back into a beaker with distilled water.

Chironomid, *Chaoborus*, Acaridae, and Simuliidae fragments were picked from the residue in a Bogorov tray using a dissecting microscope. Head capsules and fragments were transferred to a water drop on a coverslip using forceps. Once the coverslips were dry, they were mounted onto glass slides using Entellan mounting medium.

Identification of the insect fragments was done at 100-400x magnification using Olympus BH-2 and Olympus BX40 compound microscopes. Head capsules that contained less than half of a mentum were not counted, those retaining exactly half were counted as one half and those with more than half were counted as one. Identified species were then grouped using Barley's (2004) classification model. The following taxa were later regrouped to run the midge-inferred temperature reconstructions:

From Bullwinkle Lake, *Corynocera oliveri* type, Tanytarsina and *Tanytarsus* were grouped into Tanytarsina, *Micropsectra* and *Micropsectra atrofasciata/radialis* type were ungrouped from Tanytarsina and regrouped into *Micropsectra*, and *Psectrocladius (Psectrocladius) psilopterus* type and *Psectrocladius (Psectrocladius) sordidellus* type were grouped into *Psectrocladius (Psectrocladius)*.

The following taxa were ignored while running the temperature reconstructions because they were rare in the cores from Pyramid and Bullwinkle Lakes and were also not included in Barley's (2004) inference model: *Heleniella*, *Stilocladius* and Unidentifiable A from Pyramid Lake, and *Chaetocladius* type B and *Stilocladius* from Bullwinkle Lake.

4.4 <u>Data Analysis</u>

Raw data were collected and analyzed using TILIA version 2.0.b.4 (Grimm, 1993) and chironomid percentage diagrams were generated in TGView version 2.0.2 (Grimm, 2004). To differentiate zones in the core where changes in chironomid communities occurred, stratigraphically constrained incremental sum-of-squares cluster analysis was carried out using the program CONISS (Grimm, 2004).

Mean July air temperatures were reconstructed in the program C2 version 1.4.3 (Juggins, 2003-2006) using weighted averaging-partial least squares (WA-PLS) models (Lotter et al., 1999; ter Braak et al., 1993) and the surface sample data of Barley et al. (2006). These data from the Beringia training set model were taxonomically harmonized to correspond better with the data from Pyramid and Bullwinkle Lakes. This included the regrouping of *Corynocera oliveri* type and *Tanytarsus chinyensis* type with Tanytarsina and the deletion of *Rheocricotopus*. Due to these modifications, the performance values from the new model differed slightly from the original Barley et al. (2006) model. The original two-component WA-PLS model of Barley et al. (2006) yielded, r^2boot = 0.818 and RMSEP = 1.46°C. The performance values for the new model are r^2boot = 0.821 and RMSEP = 1.44°C.

Chapter V

RESULTS

5.1 Pyramid Lake

5.1.1 Sediment Lithology

Mazzucchi et al. (2003) used core PYR3 to construct the stratigraphy of the sediments from Pyramid Lake (Figure 5.1). PYR3 begins at 0 cm and ends at 395 cm, the bottom of the core.

The bottom sediment (395 cm to about 248 cm) consists of light gray diamicton, which is made up of inorganic silt and clay with angular sand to cobble size clasts. These sediments were likely deposited by a retreating glacier in the late Pleistocene. Midges were not present in the majority of this section. The remainder of the core (about 248 cm to 0 cm) is composed mainly of dark organic silt/clay, which was probably formed by the accumulation of biological material and clastic sediment (Mazzucchi et al., 2003). Midges appeared in the record at about 260 cm, and retained a significant presence throughout the rest of the core.

A thin layer of pyroclastic sand occurs at 242 cm and is AMS radiocarbon dated at 9,600 ^{14}C yr BP (approximately 10,810 cal. yr BP). The layer is one centimeter thick and, according to lithoprobe analysis, is well sorted with no clay and has a mafic mineralogy that is similar to basalt. Since the drainage basin for Pyramid Lake does not contain any basalt, the deposit is likely a pyroclastic ejecta that has not been documented in the region. A lighter colored tephra layer is also present directly below the ejecta, however it is so thin that it could not be isolated for testing. A possible source for the ejecta and tephra is Mount Edziza (Mazzucchi et al., 2003).

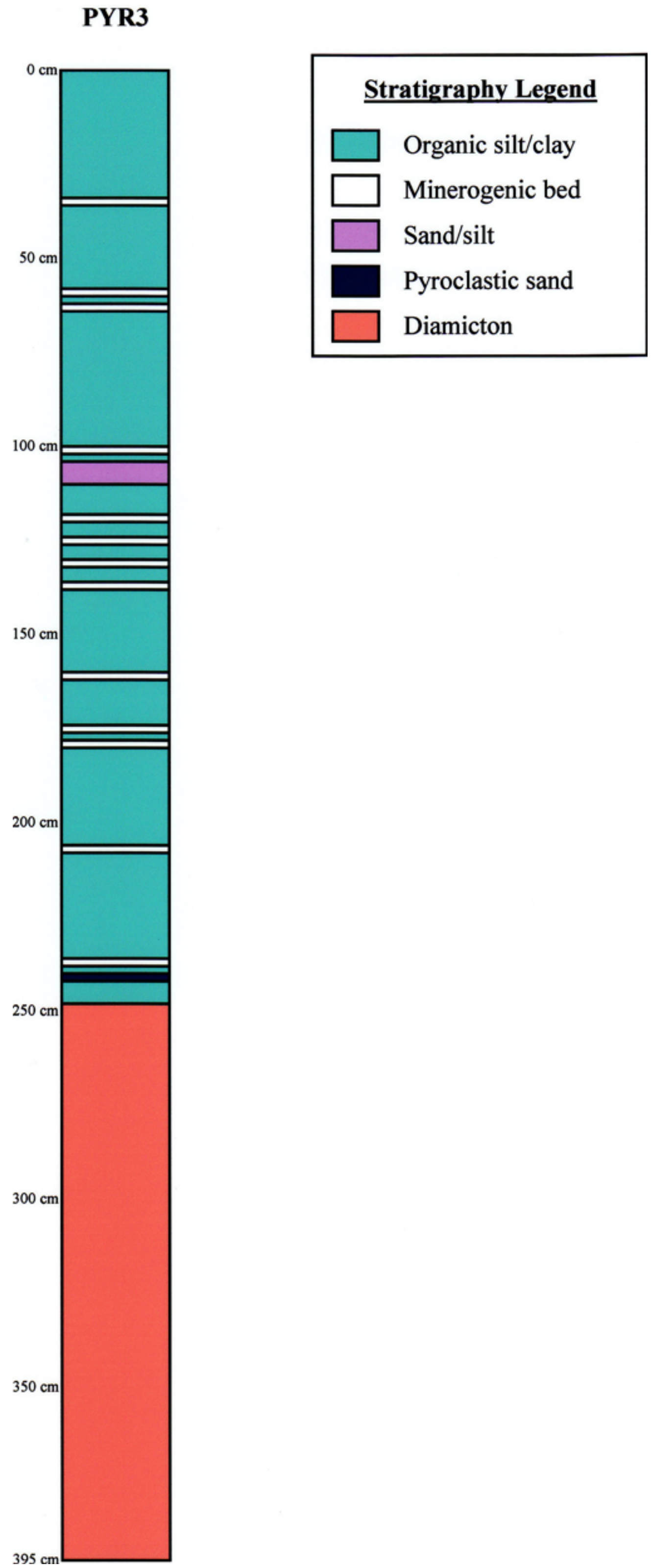

Figure 5.1: Stratigraphy of PYR3, the Pyramid Lake core (Mazzucchi et al., 2003).

A small sand/silt layer is also present in the organic silt/clay section at approximately 110-104 cm. In addition, laminae of light-coloured minerogenic sediments, which are likely allochthonous in origin, are interspersed throughout the organic silt/clay. These minerogenic layers most likely record terrestrial slope erosion triggered by large rainstorms, which delivered coarse sediment to the lake (Mazzucchi et al., 2003).

5.1.2 Chronology

Mazzucchi et al. (2003) obtained four samples for AMS radiocarbon dating from Pyramid Lake (Table 5.1). Sedimentation rate curves are relatively uniform and linear interpolation was employed to assign dates throughout the length of the PYR3 core.

Table 5.1: AMS radiocarbon dates for Pyramid Lake (Mazzucchi et al., 2003).

Core	Depth (cm)	Laboratory number	Age (^{14}C yr BP)	Calibrated age (cal. yr BP) (2 sigma)	Relative area under distribution	Material dated
PYR3	73	AA36379	2,560 ± 45	2,765-2,684	0.988	wood
				2,487-2,479	0.012	
PYR3	93	AA36380	3,555 ± 65	4,071-4,046	0.021	wood
				4,034-4,034	0.001	
				3,988-3,685	0.962	
				3,662-3,642	0.016	
PYR2	160	BGS2158	5,820 ± 130	6,907-6,379	0.964	wood
				6,373-6,311	0.036	
PYR3	241	AA36381	9,500 ± 65	11,091-10,934	0.368	wood
				10,932-10,919	0.009	
				10,910-10,634	0.557	
				10,631-10,578	0.066	

5.1.3 Midge Stratigraphy

Figure 5.2 shows the stratigraphic diagram portraying the percentage of total identifiable Chironomidae in Pyramid Lake. Taxa are ranked in accordance with their temperature optima, from cold-tolerant to warm-adapted (Barley et al., 2006). For those species with unknown temperature optima, their stratigraphies are attached to the end of the diagram.

Forty-three midge taxa were identified from the Pyramid Lake sediments. One particular group of chironomids, termed Unidentifiable A, could not be identified, but is likely a member of the subfamily Orthocladiinae (Figure 5.3a & 5.3b). Several possibilities were considered before classifying it as an unidentifiable. For example, *Parametriocnemus* has similar double ventromental plates. The pale median tooth and well-developed ventromental plates resemble *Chaetocladius*. Some *Parakiefferiella* and *Acricotopus* also bear a resemblance to the unknown species, but have smaller ventromental plates; however, the antennal pedestal present on Unidentifiable A is not usually so prominent in Orthocladiinae species.

Three distinct zones and two subzones were recognized in the core from Pyramid Lake through CONISS and visual inspection (Table 5.2). Cold-tolerant midge taxa dominate the core. Warm-adapted species that are present occur in low abundances.

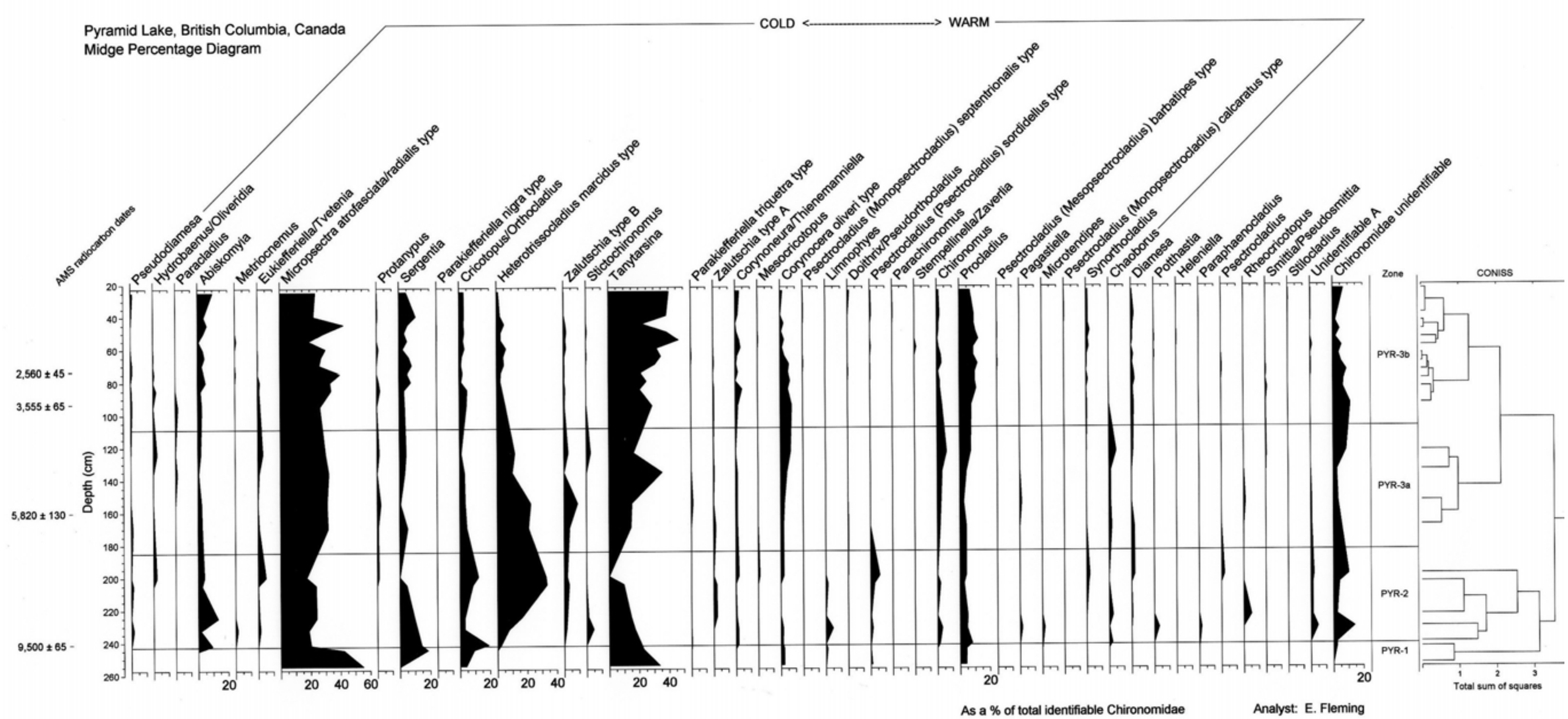

Figure 5.2: A midge stratigraphy for Pyramid Lake. Taxon abundances are expressed as a percentage of the total identifiable chironomids. Species are ordered in accordance with their temperature optima presented in Barley et al. (2006).

|---------|
10 micrometers

Figure 5.3a: Photograph of the head capsule of Unidentifiable A from Pyramid Lake (Interval pyr3-170, Slide 2/3, Coordinates 149.8, 14.7).

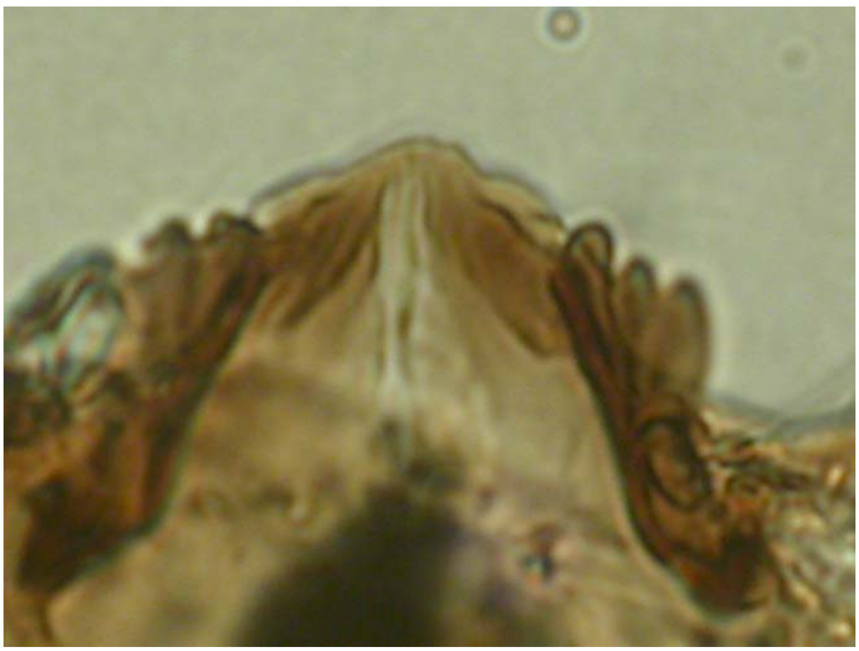

|-------------------|
5 micrometers

Figure 5.3b: Photograph of the mentum of Unidentifiable A from Pyramid Lake (Interval pyr3-170, Slide 2/3, Coordinates 149.8, 14.7).

Table 5.2: Zonation of the Pyramid Lake chironomid stratigraphy.

Chironomid assemblage zone	Depth (cm)	Calibrated Age (cal. yr BP)
PYR-3b	25-109	900-4,500
PYR-3a	109-185	4,500-7,900
PYR-2	185-243	7,900-10,900
PYR-1	243-255	10,900-11,500

5.1.3.1 <u>Zone PYR-1</u> (255-243 cm, 11,500-10,900 cal. yr BP)

Micropsectra atrofasciata/radialis type is the dominant midge species, representing ~25-55% of PYR-1. Species from the Subtribe Tanytarsina are also prominent at ~25-35%. Other common taxa include *Sergentia* (<20%) and *Cricotopus/Orthocladius* (~5-20%). Less abundant midges (<10%) include *Abiskomyia*, *Heterotrissocladius marcidus* type, *Parakiefferiella triquetra* type, *Corynoneura/Thienemanniella* type, *Limnophyes*, *Chironomus*, *Procladius*, *Microtendipes*, *Paraphaenocladius* and *Psectrocladius*. The abundance of *Procladius* remains consistent throughout the core.

5.1.3.2 <u>Zone PYR-2</u> (243-185 cm, 10,900-7,900 cal. yr BP)

There is a dramatic increase in *Heterotrissocladius marcidus* type (~5-35%) and a significant decrease in *Micropsectra atrofasciata/radialis* type (~20-30%). These species, as well as Tanytarsina which has also decreased (~5-20%) from PYR-1, are the dominant taxa in PYR-2. Both *Sergentia* and *Cricotopus/Orthocladius* reach their greatest abundance where PYR-1 transitions to PYR-2. After the peaks occur, their abundances decrease slightly and remain fairly level throughout the remainder of the core. This is also the point at which *Heterotrissocladius marcidus* type begins to increase considerably. *Heterotrissocladius marcidus* type reaches its maximum abundance in PYR-2 at 205 cm. From here on, its presence throughout the core decreases. This is also the point at which Tanytarsina is at its lowest abundance (<5%) for the entire core. *Abiskomyia* also reaches its maximum (~15%) in this zone. From here it decreases to <5% and remains that way through the remainder of the core. Low counts (<10%) make up the remaining taxa and include *Pseudodiamesa, Hydrobaenus/Oliveridia*, *Metriocnemus*, *Eukiefferiella/Tvetenia*, *Protanypus*, *Zalutschia* type B, *Stictochironomus*, *Parakiefferiella triquetra* type, *Zalutschia* type A, *Corynoneura/Thienemanniella*, *Mesocricotopus*, *Corynocera oliveri* type, *Limnophyes*, *Doithrix/Pseudorthocladius*, *Psectrocladius (Psectrocladius) sordidellus* type, *Chironomus*, *Procladius*, *Pagastiella*, *Microtendipes*, *Synorthocladius*, *Chaoborus*, *Diamesa*, *Potthastia*, *Paraphaenocladius*, *Psectrocladius*, *Rheocricotopus* and Unidentifiable A.

5.1.3.3 <u>Zone PYR-3a</u> (185-109 cm, 7,900-4,500 cal. yr BP)

Micropsectra atrofasciata/radialis type, *Heterotrissocladius marcidus* type and Tanytarsina remain the dominant taxa in PYR-3a. *Micropsectra atrofasciata/radialis* type has increased slightly (~30%) and remains uniform throughout this zone. *Heterotrissocladius marcidus* type continues to decrease throughout PYR-3a, from ~25-10%. Tanytarsina increases to form a peak (~40%), and follows by decreasing to form a trough (~25%). From here the assemblage starts to increase at a more moderate rate. The remaining taxa all occur at low abundances (<10%) and include *Pseudodiamesa*, *Hydrobaenus/Oliveridia*, *Paracladius*, *Abiskomyia*, *Eukiefferiella/Tvetenia*, *Protanypus*, *Sergentia*, *Cricotopus/Orthocladius*, *Zalutschia* type B, *Stictochironomus*, *Parakiefferiella triquetra* type, *Zalutschia* type A, *Corynoneura/Thienemanniella*, *Mesocricotopus*, *Corynocera oliveri* type, *Psectrocladius (Psectrocladius) sordidellus* type, *Chironomus*, *Procladius*, *Pagastiella*, *Synorthocladius*, *Chaoborus*, *Diamesa*, *Psectrocladius*, *Rheocricotopus*, *Smittia/Pseudosmittia* and Unidentifiable A.

5.1.3.4 <u>Zone PYR-3b</u> (109-25 cm, 4,500-900 cal. yr BP)

This zone is characterized by the fluctuations of the two dominant taxa, *Micropsectra atrofasciata/radialis* type and Tanytarsina. Several peaks are present within the two taxa in PYR-3b. *Micropsectra atrofasciata/radialis* type exhibits a low of ~20% and a high of ~40%. Tanytarsina displays a low and a high of ~25% and ~50%, respectively. *Heterotrissocladius marcidus* type levels off and remains at ~5%. *Procladius* increases slightly and remains constant (~10%) throughout the zone. Low abundances comprise the remaining taxa and include *Pseudodiamesa*, *Hydrobaenus/Oliveridia*, *Paracladius*, *Abiskomyia*, *Metriocnemus*, *Eukiefferiella/Tvetenia*, *Protanypus*, *Sergentia*, *Parakiefferiella nigra* type, *Cricotopus/Orthocladius*, *Zalutschia* type B, *Stictochironomus*, *Parakiefferiella triquetra* type, *Zalutschia* type A, *Corynoneura/Thienemanniella*, *Mesocricotopus*, *Corynocera oliveri* type, *Psectrocladius (Monopsectrocladius) septentrionalis* type, *Doithrix/Pseudorthocladius*, *Psectrocladius (Psectrocladius) sordidellus* type, *Parachironomus*, *Stempellinella/Zavrelia*, *Chironomus*, *Psectrocladius (Mesopsectrocladius) barbatipes* type, *Psectrocladius (Monopsectrocladius) calcaratus* type, *Synorthocladius*, *Chaoborus*, *Diamesa*, *Potthastia*, *Heleniella*, *Psectrocladius*, *Smittia/Pseudosmittia*, *Stilocladius* and Unidentifiable A.

5.1.4 Temperature Reconstructions

The temperature reconstruction for Pyramid Lake reveals fluctuations in summer Holocene air temperatures ranging from 8.5-11°C (Figure 5.4a & 5.4b). However, when a LOWESS smoother is overlaid on the temperature curve, the inferred mean July air temperatures drop slightly to range from 8.5-10.5°C. Further discussions are based on the LOWESS smoothed temperatures as opposed to the raw temperature curve.

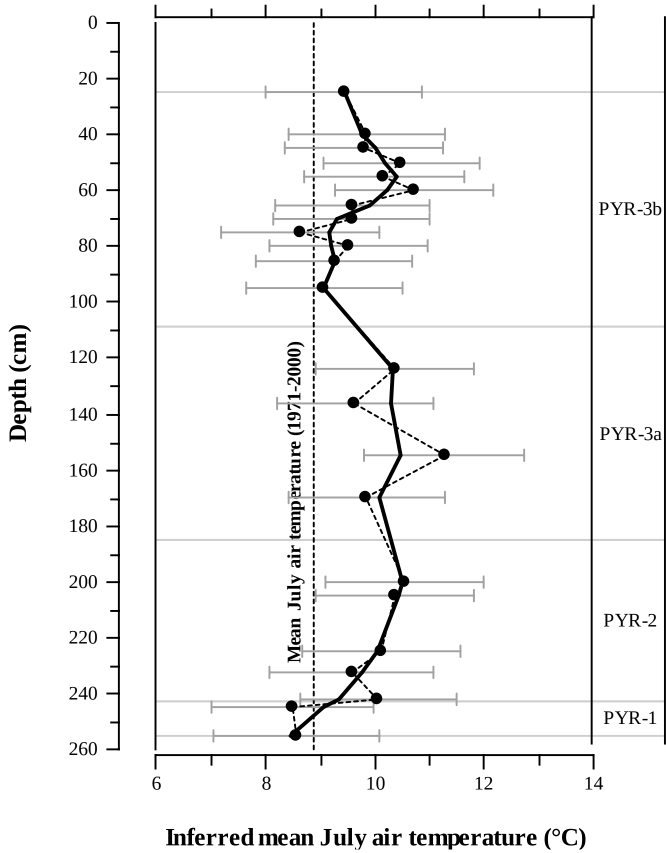

Figure 5.4a: Mean July air temperatures as inferred by WA-PLS as a function of depth for Pyramid Lake. A LOWESS smooth (thick line) is overlaid on the temperature curve (thin line). Error bars correspond to the sample specific estimated standard errors. The corrected daily mean July air temperature (1971-2000) of 8.9°C is represented by the dashed line.

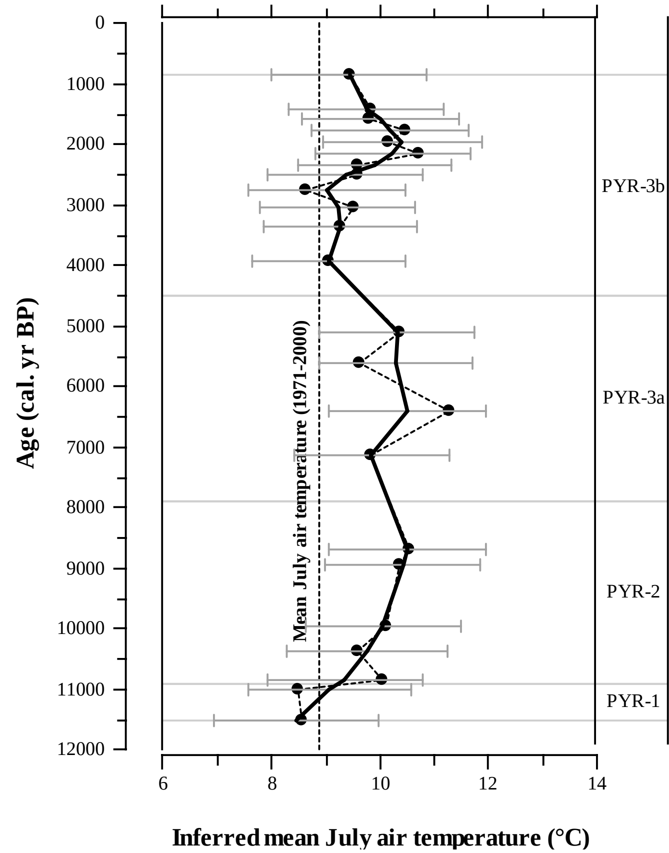

Figure 5.4b: Mean July air temperatures as inferred by WA-PLS as a function of age for Pyramid Lake. A LOWESS smooth (thick line) is overlaid on the temperature curve (thin line). Error bars correspond to the sample specific estimated standard errors. The corrected daily mean July air temperature (1971-2000) of 8.9°C is represented by the dashed line.

The corrected modern mean July air temperature (1971-2000) at Pyramid Lake is 8.9°C. This fits into the lower-most range of mean July air temperatures inferred by WA-PLS, and may be an indication that the Beringia training set model provided by Barley et al. (2006) overestimates temperatures in this region.

5.1.4.1 Zone PYR-1 (255-243 cm, 11,500-10,900 cal. yr BP)

The coldest mean July air temperatures occur in PYR-1 during the early Holocene, with a steady increase from 8.5-9.5°C.

5.1.4.2 Zone PYR-2 (243-185 cm, 10,900-7,900 cal. yr BP)

Temperatures continue to rise in PYR-2 from 9.5°C until they reach a maximum of 10.5°C at 8,700 cal. yr BP. This early Holocene warming trend may signify the presence of the Milankovitch thermal maximum. Temperatures decrease slightly at the end of the zone from 10.5°C to slightly above 10°C.

5.1.4.3 Zone PYR-3a (185-109 cm, 7,900-4,500 cal. yr BP)

The temperatures in PYR-3a, the mid-Holocene, display minor fluctuations, however the general trend appears to be a decrease from between 10-10.5°C to 9.5°C.

5.1.4.4 Zone PYR-3b (109-25 cm, 4,500-900 cal. yr BP)

Temperatures fluctuate in the late Holocene from 9°C to slightly below 10.5°C. Overall, temperatures in PYR-3 cool from 9.5-9°C, and remain this way from 3,900-2,750 cal. yr BP. This is followed by an increase in temperature to 10.5°C at 2,000 cal. yr BP. From here, temperatures drop back to 9.5°C at the end of the zone.

5.2 Bullwinkle Lake

5.2.1 Sediment Lithology

Two overlapping cores (BULL1 and BULL2), in addition to the surface core, were used to construct the stratigraphy of the sediments from Bullwinkle Lake (Figure 5.5). The surface core starts at 0 cm and is 35 cm long. BULL1 begins at 42 cm and ends at 139 cm. BULL2 overlaps BULL1 and starts at 111 cm and ends at 170 cm, the bottom of the core.

The bottom-most layers of both cores (139-136 cm in BULL1 and 170-136 cm in BULL2) are made up of grayish-brown silty-clay. It was likely deposited in the late Pleistocene when the glaciers were retreating. No midges were found in this section.

Immediately above the clay in BULL1 and BULL2 is a deposit (Figure 5.6) consisting of whitish-brown, fine-grained pyroclastic tephra (136-132 cm), and directly above this is a layer of dark black, coarse grained pyroclastic ejecta (132-120 cm). This pyroclastic layer was deposited just prior to 9,500^{14}C yr BP (approximately 10,750 cal. yr BP). The ejecta from Bullwinkle Lake was sent to the University of Alberta for probing. Analysis indicated that it is phenolitic in composition with 59-60 wt.% silicon dioxide and abundant sodium, potassium and iron. Its chemical composition is similar to two early Holocene ejectas and tephras found in several lakes near Dease Lake and Finlay River in northern British Columbia. These have a minimum age of 9,180 ^{14}C yr BP (10,220-10,560 cal. yr BP) and likely originate from two closely spaced eruptions in northwestern British Columbia, either from Hoodoo Mountain, Mount Edziza, Heart Peaks or Level Mountain (Lakeman, 2006). The tephra from Bullwinkle Lake was also sent to the University of Calgary for analysis, however the results came back as

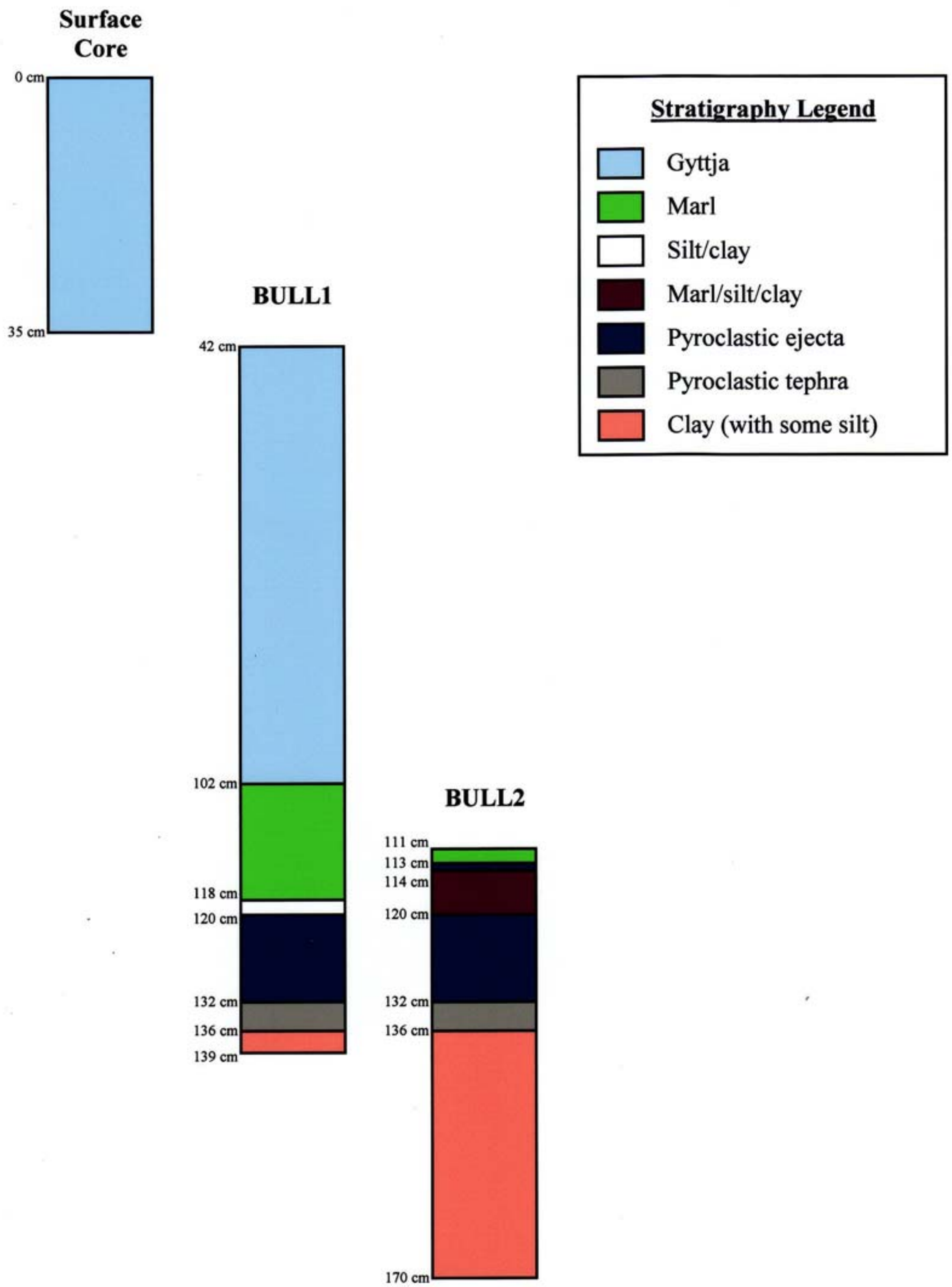

Figure 5.5: Stratigraphy of the Bullwinkle Lake cores (surface core, BULL1 and BULL2).

Figure 5.6: Photograph of the pyroclastic ejecta and tephra from cores BULL1 (top) and BULL2 (bottom) from Bullwinkle Lake. The tops of the cores are to the left and the bottoms of the cores are to the right. The pyroclastic ejecta is the dark black coarsely grained material and occurs at a depth of 120 to 132 centimeters. The pyroclastic tephra is the white to light brown finely grained material and occurs at a depth of 132 to 136 centimeters (located to the right of the pyroclastic ejecta in the photograph).

inconclusive. The pyroclastic layer found in Bullwinkle Lake is probably of the same origin as the pyroclastic sand found in Pyramid Lake.

Directly above the ejecta in BULL1 is a thin layer of light brown silt/clay (120-118 cm) followed by a light brown marl layer (118-102 cm). Marl is calcium carbonate-rich mud and could possibly contain old carbon. In BULL2, also immediately above the ejecta, is a layer of marl/silt/clay (120-114 cm), which may be a combination of the silt/clay and marl layers found in BULL1.

BULL2 contains a fine layer (114-113 cm) of the same pyroclastic ejecta found at 132-120 cm in both cores. Since the layer at 114 cm in BULL2 is not present in BULL1, and because it appears to have the same composition as the layer at 132 cm, it may be that the thin deposit was washed into the lake from the surrounding terrain years after the eruption occurred and coated the region.

The top segment (113-111 cm) of BULL2 reveals a small layer of light brown marl, which is consistent with the deposit found in BULL1 at 118-102 cm. The sediments in the top portion (102-42 cm) of BULL1 consist of dark brown gyttja. The surface core (35-0 cm) is also composed of dark brown gyttja. There is a small gap in the stratigraphy (42-35 cm), between BULL1 and the surface core; however, it can be assumed that it also consists mainly of dark brown gyttja.

All the sediments that were deposited above the tephra and ejecta represent the accumulation of biological material and clastic sediment. Midge analysis was performed on this entire section.

5.2.2 Chronology

Eight samples were obtained for AMS radiocarbon dating from Bullwinkle Lake (Table 5.3). Sedimentation rates are not uniform and there are several inversions in the AMS radiocarbon dates (Figure 5.7a). Regression analysis yields the following equation relating depth and age, where x=depth (cm) and y=age (cal. yr BP) (Figure 5.7b):

$$y = 166.81 - 14.09x + 0.61x^2$$

A linear relationship is displayed between depth and age for the first eleven and a half cm.

A limitation to this calculated regression model is the possibility that it underestimates ages. Evidence for this is shown in the date of a pyroclastic sand layer found in both Pyramid and Bullwinkle Lakes. The sand layer occurs in Pyramid Lake just prior to 10,810 cal. yr BP and just prior to 10,750 cal. yr BP in Bullwinkle Lake; however, after regression analysis is performed on the dates for Bullwinkle Lake, the pyroclastic sand yields a date of just prior to 7,300 cal. yr BP.

Table 5.3: AMS radiocarbon dates for Bullwinkle Lake.

Core	Depth (cm)	Laboratory number	Age (^{14}C yr BP)	Calibrated age (cal. yr BP) (2 sigma)	Relative area under distribution	Material dated
BULL1	48-51	44522	1,730 ± 20	1,569-1,700	1.000	aquatic leaf fragment
						herbaceous woody stem fragments
BULL1 & BULL3	72-76	44523	1,205 ± 40	1,008-1,028	0.030	*Abies lasiocarpa* needles
				1,053-1,191	0.804	herbaceous woody stem fragments
				1,197-1,262	0.166	
BULL3	80-81	44524	4,270 ± 20	4,830-4,858	1.000	herbaceous woody stem fragment
BULL3	98-99	44525	4,780 ± 25	5,471-5,557	0.849	herbaceous woody stem fragment
				5,569-5,588	0.151	plant fragment
BULL3	109-110	44526	3,920 ± 20	4,290-4,423	1.000	herbaceous woody stem fragments
BULL3	110-111	44527	3,895 ± 20	4,250-4,273	0.085	herbaceous woody stem fragments
				4,284-4,415	0.915	
BULL3	111-112	44528	3,930 ± 20	4,293-4,428	1.000	Bryophyte stem fragments
						herbaceous woody stem fragment
BULL1	119-120	44529	9,495 ± 30	10,607-10,616	0.007	*Carex* trigonous type achenes
				10,657-10,801	0.739	
				10,851-10,863	0.012	
				10,956-11,067	0.242	

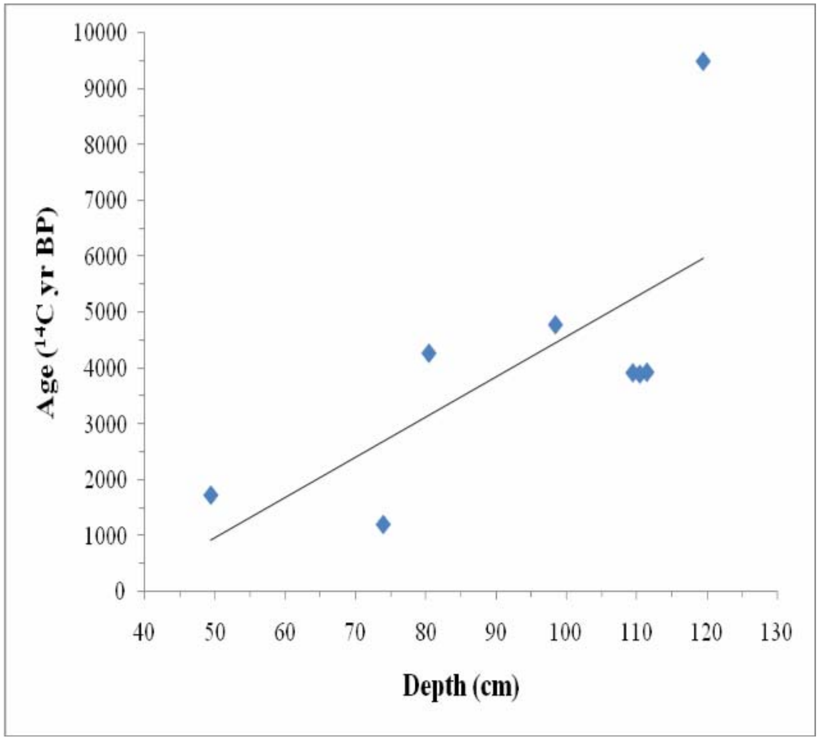

Figure 5.7a: The AMS radiocarbon dates obtained from Bullwinkle Lake as a function of depth.

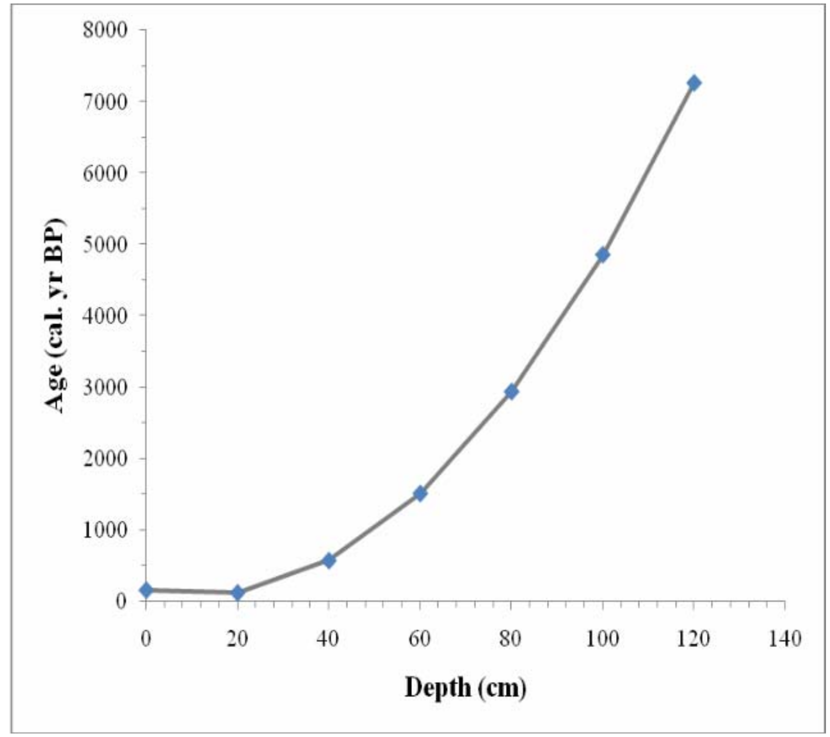

Figure 5.7b: The age-depth regression model for Bullwinkle Lake. Age is measured in calibrated years, based on the original AMS radiocarbon dates. Regression analysis yields the following equation: $y = 166.81 - 14.09x + 0.61x^2$, , where x = depth (cm) and y = age (cal yr BP).

5.2.3 Midge Stratigraphy

The percentage of total identifiable Chironomidae in Bullwinkle Lake is depicted in a stratigraphic diagram (Figure 5.8). Taxa are ranked in accordance with their temperature optima, from cold-tolerant to warm-adapted (Barley et al., 2006). For those whose temperature optima is unknown, stratigraphies are attached to the end of the diagram.

Thirty-four midge taxa were identified from the Bullwinkle Lake sediments. Two distinct zones were recognized in the core through CONISS and visual inspection (Table 5.4). Cold-tolerant midge taxa dominate the core; however, warm-adapted taxa have a greater presence with higher abundances than were found in Pyramid Lake.

5.2.3.1 Zone BULL-1 (120-102 cm, 7,300-5,100 cal. yr BP)

The Subtribe Tanytarsina is the dominant taxon, accounting for ~25-40% of BULL-1, the highest it occurs throughout the entire core. Other common taxa include *Tanytarsus* (~5-20%), *Psectrocladius (Psectrocladius) sordidellus* type (~10-20%) and species from the Tribe Pentaneurini (~5-15%). Interestingly, the peaks that *Tanytarsus* forms correspond to the troughs of Tanytarsina and vice versa throughout BULL-1. Both *Cricotopus/Orthocladius* and *Corynoneura/Thienemanniella* have moderate abundances (~25% and ~10%, respectively) at the deepest portion of the zone, and then suddenly decrease to <5%. They remain at these abundances for the remainder of the core. The remaining taxa are present at low abundance (<10%) including *Paracladius*, *Sergentia*, *Corynocera oliveri* type, *Psectrocladius (Monopsectrocladius) septentrionalis* type, *Corynocera ambigua* type, *Psectrocladius (Psectrocladius) psilopterus* type,

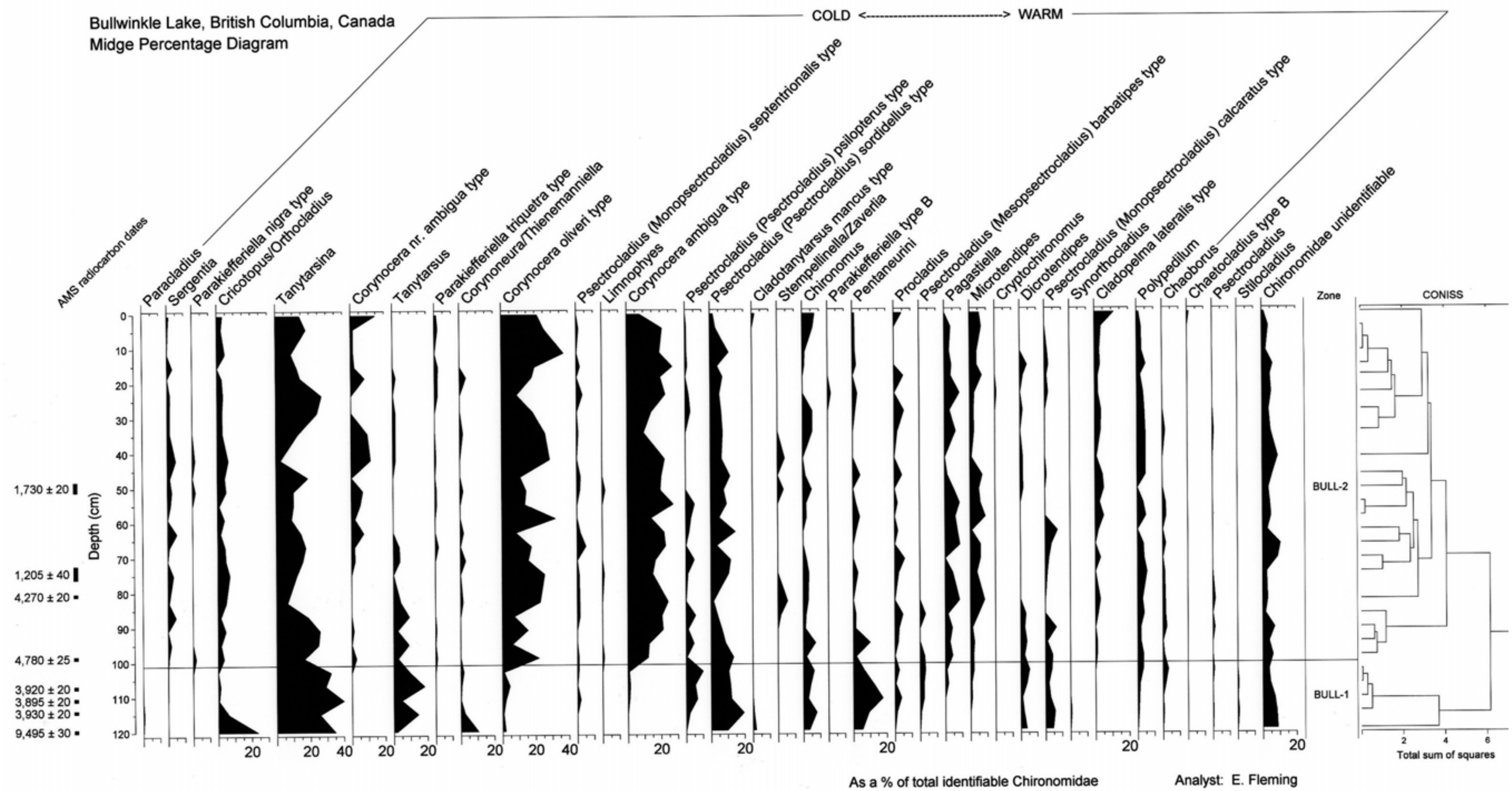

Figure 5.8: A midge stratigraphy for Bullwinkle Lake. Taxon abundances are expressed as a percentage of the total identifiable chironomids. Species are ordered in accordance with their temperature optima presented in Barley et al. (2006).

Table 5.4: Zonation of the Bullwinkle Lake chironomid stratigraphy.

Chironomid assemblage zone	Depth (cm)	Calibrated Age (cal. yr BP)
BULL-2	0.5-102	0-5,100
BULL-1	102-120	5,100-7,300

Cladotanytarsus mancus type, *Chironomus*, *Procladius*, *Psectrocladius (Mesopsectrocladius) barbatipes* type, *Pagastiella*, *Microtendipes*, *Dicrotendipes*, *Psectrocladius (Monopsectrocladius) calcaratus* type, *Synorthocladius*, *Polypedilum*, *Chaoborus*, *Psectrocladius* and *Stilocladius*.

5.2.3.2 <u>Zone BULL-2</u> (102-0.5 cm, 5,100-0 cal. yr BP)

There is a significant decrease in Tanytarsina (~5-25%) and considerable increases in *Corynocera oliveri* type (~10-35%) and *Corynocera ambigua* type (~10-25%). These three taxa dominate BULL-2 and exhibit large fluctuations throughout the zone. *Psectrocladius (Psectrocladius) sordidellus* type shows a distinct trend in abundance (~5-20%), whereas *Tanytarsus* and Pentaneurini both start to decrease above the BULL-1/BULL-2 boundary. They eventually both level off to <5% and stay that way throughout the rest of the core. *Corynocera nr. ambigua* first appears at 99 cm; however, it does not make a substantial appearance until 63 cm. From here on it fluctuates between ~0-15% through the rest of the core. Low abundances comprise the remaining taxa and include *Sergentia*, *Parakiefferiella nigra* type, *Cricotopus/Orthocladius*, *Parakiefferiella triquetra* type, *Corynoneura/Thienemanniella*, *Psectrocladius(Monopsectrocladius) septentrionalis* type, *Limnophyes*, *Psectrocladius (Psectrocladius) psilopterus* type, *Cladotanytarsus mancus* type, *Stempellinella/Zavrelia*, *Chironomus*, *Parakiefferiella* type B, *Procladius*, *Psectrocladius (Mesopsectrocladius) barbatipes* type, *Pagastiella*, *Microtendipes*, *Cryptochironomus*, *Dicrotendipes*, *Psectrocladius (Monopsectrocladius) calcaratus* type, *Cladopelma lateralis* type, *Polypedilum*, *Chaoborus*, *Chaetocladius* type B and *Psectrocladius*.

5.2.4 <u>Temperature Reconstructions</u>

Reconstructed Holocene air temperatures for Bullwinkle Lake fluctuate little and range from 11-13°C (Figure 5.9a & 5.9b). However, when a LOWESS smoother is overlaid on the temperature curve, the inferred mean July air temperatures range from 11°C to slightly below 13°C. Further discussions are based on the LOWESS smoothed temperatures as opposed to the raw temperature curve.

The corrected modern mean July air temperature (1971-2000) at Bullwinkle Lake is 9.8°C. This does not fit into the range of mean July air temperatures inferred by WA-PLS, and may be an indication that the Beringia training set model provided by Barley et al. (2006) overestimates temperatures in this region.

5.2.4.1 Zone BULL-1 (120-102 cm, 7,300-5,100 cal. yr BP)

Mean July air temperatures increase from a minimum of 11°C to 12.5°C in BULL-1.

5.2.4.2 Zone BULL-2 (102-0.5 cm, 5,100 -0 cal. yr BP)

In BULL-2, temperatures average 12.5°C until 1,700 cal. yr BP. From here, temperatures rise to a maximum of just under 13°C at 1,200 cal. yr BP. A cooling trend then occurs until 850 cal. yr BP when temperatures drop to 12.5°C. Few fluctuations occur throughout the remainder of this zone.

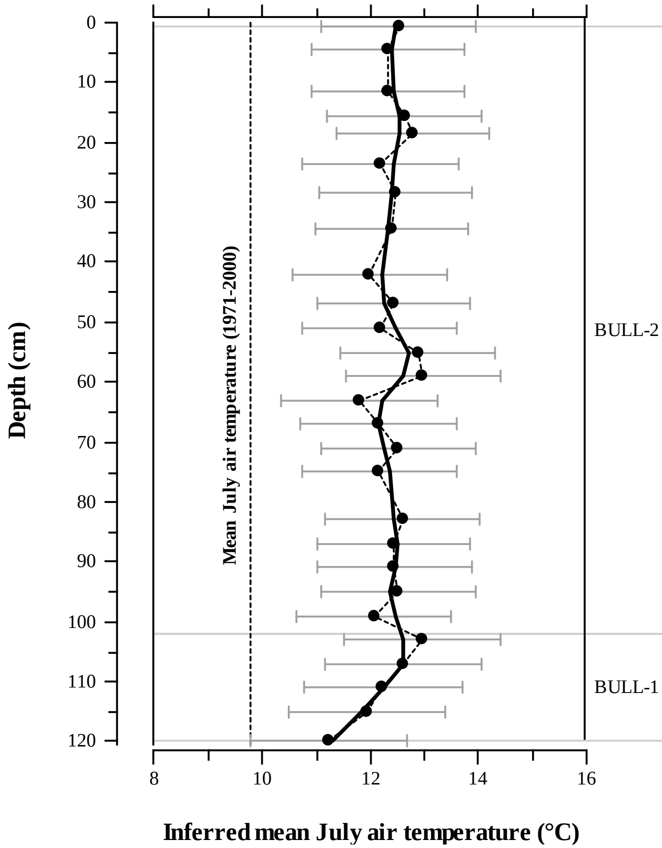

Figure 5.9a: Mean July air temperatures as inferred by WA-PLS as a function of depth for Bullwinkle Lake. A LOWESS smooth (thick line) is overlaid on the temperature curve (thin line). Error bars correspond to the sample specific estimated standard errors. The corrected daily mean July air temperature (1971-2000) of 9.8°C is represented by the dashed line.

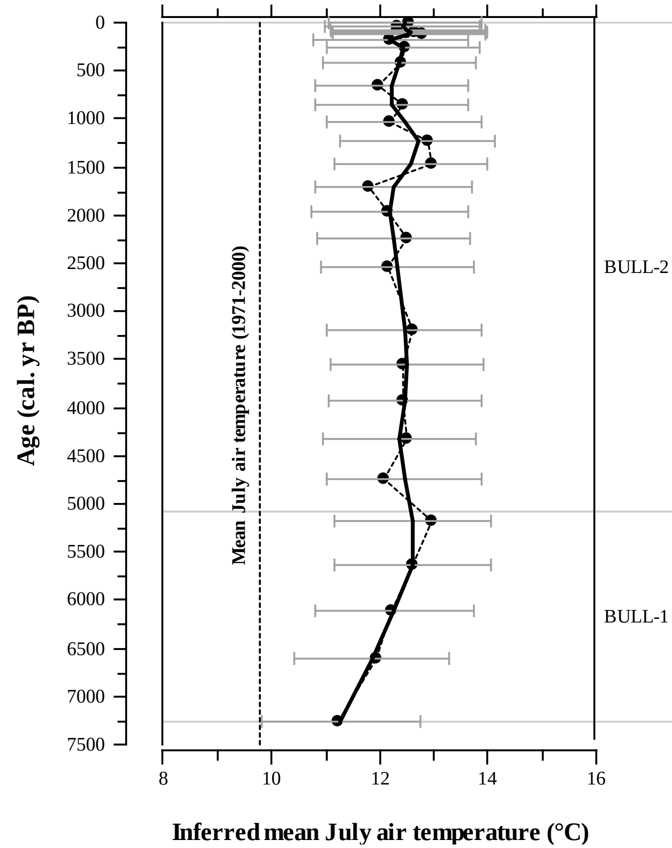

Figure 5.9b: Mean July air temperatures as inferred by WA-PLS as a function of age for Bullwinkle Lake. A LOWESS smooth (thick line) is overlaid on the temperature curve (thin line). Error bars correspond to the sample specific estimated standard errors. The corrected daily mean July air temperature (1971-2000) of 9.8°C is represented by the dashed line.

Chapter VI

DISCUSSION

6.1 Pyramid Lake

The Pyramid Lake record provides the first midge-inferred mean July air temperatures for northern British Columbia. Integrating this reconstruction with Mazzucchi et al.'s (2003) pollen analysis provides a complete Holocene summer palaeoclimatic record for Pyramid Lake.

6.1.1 Lithology

The bottom-most sediments of PYR3, the core from Pyramid Lake (Figure 5.1), consist of diamicton that was deposited by a late Pleistocene retreating glacier probably around 12,800 cal. yr BP (Mazzucchi et al., 2003). Midges were only found in the uppermost 12 cm of this section, presumably due to the lack of a hospitable environment. Directly above this layer is organic silt/clay which extends throughout the remainder of the Holocene. This section represents the slow accumulation of biological material and clastic sediments. Midge communities were present throughout this entire section, with the exception of the thin layer of pyroclastic deposit.

The pyroclastic sand was deposited at about 10,810 cal. yr BP. Mazzucchi et al. (2003) suggest the Edziza plateau as a possible source for the volcanic eruption. A similar, but thicker, deposit also occurs in Bullwinkle Lake at around 10,750 cal. yr BP. These deposits likely originate from the same eruption.

A small sand/silt layer (approximately 4,400 cal. yr BP) and several interspersed laminae of minerogenic sediments also occur in the organic silt/clay. The minerogenic layers are thought to be allochthonous, and originate from eroded hill-slope sediments deposited during high-intensity rainstorms (Mazzucchi et al., 2003).

6.1.2 Chronology

In Pyramid Lake there are no inversions evident in the AMS radiocarbon dates (Table 5.1). Sedimentation rate curves reveal a relatively uniform sedimentation rate.

6.1.3 Climate

The midge-inferred temperature reconstruction for Pyramid Lake reveals an oscillating pattern of summer temperatures ranging from 8.5-10.5°C (Figure 5.4a & 5.4b) with cold-tolerant midge taxa dominating the core (Figure 5.2).

6.1.3.1 The Early Holocene

Pyramid Lake's palaeoclimatic record begins around 11,500 cal. yr BP, shortly after the glaciers retreated. From 11,500-7,900 cal. yr BP (PYR-1 & PYR-2) mean July air temperatures rise from 8.5°C, the coldest recorded period, to 10.5°C, the warmest observed period.

Early in PYR-1, when temperatures are near 8.5°C, *Micropsectra atrofasciata/radialis* type and species from the Subtribe Tanytarsina are the dominant taxa. *Micropsectra atrofasciata/radialis* type is a cold stenotherm and typically lives in ultra-oligotrophic, cold arctic or alpine lakes (Brooks et al., 2007). Tanytarsina is also a cold-tolerant taxon (Barley et al., 2006), and both of these assemblages are indicative of the cold temperatures present at the beginning of the early Holocene in Pyramid Lake. Other common taxa include *Sergentia* and *Cricotopus/Orthocladius*, whose abundances peak during the transition from PYR-1 to PYR-2 at 10,900 cal. yr BP. These are also cold stenotherms and are found in lakes from subarctic to temperate and montane regions.

Temperatures reach a maximum of 10.5°C at 8,700 cal. yr BP in PYR-2. *Heterotrissocladius marcidus* type, typically found in cold oligotrophic lakes, first appears and then dominates for the remainder of the early Holocene. *Micropsectra atrofasciata/radialis* type and Tanytarsina also have a significant presence, although their abundances have decreased from PYR-1. The rising temperatures may have had an effect on their existence in the region. Other cold-tolerant species whose abundances have decreased are *Sergentia* and *Cricotopus/Orthocladius*.

The early Holocene warming trend revealed in PYR-1 and PYR-2 may signify the presence of the Milankovitch thermal maximum (MTM). Just as several researchers (Ritchie, 1985; Kaufman et al., 2004) have suggested, summer temperatures were on the order of 10% warmer than present, with a corrected daily mean July air temperature (1971-2000) of 8.9°C. However this inference should be interpreted with caution, because the modern summer temperature for the region fits into only the lower-most range of mean July air temperatures as inferred by WA-PLS, and may indicate that the Beringia training set model overestimates temperatures at Pyramid Lake.

At the very end of the early Holocene (8,700-7,900 cal. yr BP) temperatures begin to decrease. During this time, a cold period lasting 200 years occurred in the North Atlantic and was known as the 8,200 cal. yr BP cooling event (Hammarlund et al., 2005). Evidence from North America suggests that this cold period also occurred in the western half of the northern hemisphere (Shuman et al., 2002; Kurek et al., 2004; Yu & Eicher, 1998; Pisaric et al., 2003; von Grafenstein et al., 1998). It is debatable whether this cooling phase at Pyramid Lake is indicative of the 8,200 cal. yr BP cooling event, therefore further detailed analysis is needed on this section of the core.

6.1.3.2 <u>The Middle Holocene</u>

The middle Holocene (PYR-3a) is characterized by an overall decrease in summer temperature, with minor fluctuations, from between 10-10.5°C to 9.5°C. *Heterotrissocladius marcidus* type remains the dominant species during the transition (7,900 cal. yr BP) from the early to middle Holocene; however, its abundance significantly decreases as temperatures decline. By the end of the period (4,500 cal. yr BP) its presence in Pyramid Lake is minimal. At the same time, *Micropsectra atrofasciata/radialis* type and Tanytarsina have increased slightly and remain the dominant taxa throughout the middle Holocene.

One minor fluctuation includes a slight increase in temperature, starting at 7,100 cal. yr BP. At 5,100 cal. yr BP temperatures begin to decrease again. This temperature flux overlaps with an episode found by Mazzucchi et al. (2003) using pollen from Pyramid Lake. An elevated white spruce (*Picea glauca*) community at 5,900 cal. yr BP supported the idea of increased summer temperatures which may have caused several high-magnitude rainstorm events. This shift in climate lasted until 4,500 cal. yr BP.

6.1.3.3 <u>The Late Holocene</u>

Temperatures in the late Holocene (PYR-3b) fluctuate between 9°C and just below 10.5°C. *Micropsectra atrofasciata/radialis* type and Tanytarsina, the dominant taxa, also oscillate throughout this period. At the beginning (4,500 cal. yr BP) of the late Holocene, temperatures continue to cool from 9.5-9°C, and remain this way from 3,900-2,750 cal. yr BP. Temperatures then increase to 10.5°C by 2,000 cal. yr BP. At this time there is a distinct drop in the cold-tolerant taxon, *Micropsectra atrofasciata/radialis* type. Its abundance immediately increases again as temperatures drop back to 9.5°C by 900 cal. yr BP. After the drop in *Heterotrissocladius marcidus* type in the middle Holocene, its abundance remains minimal, but constant throughout the late Holocene. *Procladius*, one of the warmer-tolerant taxa found in mesotrophic and eutrophic lakes (Brooks et al., 2007), which has also been present in low, but steady abundances throughout the early and middle Holocene, increases slightly in the late Holocene and remains stable all through this period.

6.2 <u>Bullwinkle Lake</u>

The Bullwinkle Lake midge-inferred mean July air temperatures record provides insight into Holocene climate change in a region lacking in palaeoclimatic work. Incorporating these data with the Pyramid Lake reconstruction should help to resolve some discrepancies in the details of climate change since deglaciation in northern British Columbia.

6.2.1 <u>Lithology</u>

The bottom-most sediments of Bullwinkle Lake's cores (BULL1 and BULL2), (Figure 5.5) consist of silty-clay material, which was likely deposited in the late Pleistocene around 12,800 cal. yr BP when the area was deglaciating (Mazzucchi et al., 2003). No midges were found in this layer, as these sediments were probably deposited very rapidly and the area probably may not yet have had a suitable environment and climate for the insects. Directly above the clay is a 4 cm layer of pyroclastic tephra followed immediately by a 12 cm layer of pyroclastic ejecta (Figure 5.6). These were deposited around 10,750 cal. yr BP. These same pyroclastic layers are also found in the Pyramid Lake cores and yield a date of approximately 10,810 cal. yr BP. However the deposits in Pyramid Lake are significantly thinner than those found in Bullwinkle Lake, with the tephra being only a few millimeters thick and the ejecta measuring about 1 cm thick (Mazzucchi et al., 2003). The tephra most likely originates from the initial volcanic eruption, whereas the ejecta is probably the material expelled from the volcano thereafter.

The deposits from Pyramid and Bullwinkle Lake resemble two early Holocene ejectas and tephras found in several lakes near Dease Lake and Finlay River in northern British Columbia. These have a similar minimum age of 10,220-10,560 cal. yr BP. Possible sources for the pyroclastic material are located within the Stikine Volcanic Belt and include Mount Edziza, Hoodoo Mountain, Heart Peaks and Level Mountain (Lakeman, 2006), and are all located within a maximum distance of 400 km south-west of the lakes in northwestern British Columbia. Further research is needed in the area to determine the exact location of the eruption.

Sediments above the pyroclastic material in Bullwinkle Lake consist of silt, clay and marl followed by an extensive gyttja layer. These deposits represent the accumulation of biological material and clastic sediments as the region slowly changed from an early post-glacial landscape to the environment we see today. The presence of midges was first detected after the pyroclastic material blanketed the region and remains constant throughout the remainder of the core.

6.2.2 Chronology

In Bullwinkle Lake several inversions are evident in the AMS radiocarbon dates (Table 5.3 & Figure 5.7a). This may be caused by the location of the lake in a wind corridor in addition to it being quite shallow, with a maximum depth of less than 2 m. These combined factors would have increased sediment mixing and possible resuspension of the dating materials.

Intervals 48-51, 72-76, 80-81, 98-99, 109-110, 110-111, and 111-112 cm were all dated using unidentified herbaceous woody stem fragments that may belong to an aquatic type plant. They are potentially susceptible to the hard-water effect (Shotton, 1972) as well as old carbon contamination, which may yield other possible sources for the inversions. In the hard-water effect, aquatic plants assimilate carbon from water that contains bicarbonate derived from older sources, rather than from the atmosphere. This yields older than expected dates, sometimes by as much as several thousand years. This effect is more pronounced in areas where limestone and calcareous rocks occur. Surface and groundwater in these areas have lower $^{14}C/^{12}C$ than the atmosphere due to the free ^{14}C in bedrock solution (Bradley, 1999). However, the watershed for Bullwinkle Lake does not appear to contain significant amounts of limestone, so the hard-water effect may be insignificant.

Old carbon contamination can also occur when the geochemical balance of lakes changes through time, which means the modern chemistry of the water may not reflect conditions from the past. This was demonstrated in a study on lake sediments in southwestern New Brunswick (Karrow & Anderson, 1975). They suggested that shortly after deglaciation, lake sediments consisting of marl derived from carbonate till and bedrock were contaminated with old carbon; however, as the area became more vegetated and soils developed, the sediments became more organic and less contaminated. This caused the basal sediments to have much older dates than expected. It is not uncommon to see this effect in formerly glaciated environments where the environment immediately following deglaciation is quite different from that of today; therefore, caution should be given to interpreting basal dates on sediments (MacDonald et al., 1991). The only basal date obtained from Bullwinkle Lake is from interval 119-120 cm, directly above the pyroclastic sand. This date does not appear to have been contaminated because it closely matches the date obtained above the same material found in Pyramid Lake's sediments.

Lakes that have changed in size may have also experienced changes in the water's geochemistry (Bradley, 1999). Bullwinkle Lake shows evidence of recent beaver activity and a surface water outlet is currently dammed on its south-east end. The basin was not formed by beavers, however, the surface level of the lake may have been raised by approximately 1m throughout the Holocene. Any changes in the water's chemistry from this may be reflected in the radiocarbon dates, and might help to explain some of the apparent inversions.

Sedimentation rates for the lake were not uniform below 11.5 cm. Regression analysis was used to determine a relationship between depth and age, with the possibility that there is an underestimation of the true age of the sediments (Figure 5.7b). For example, the pyroclastic sand found in Pyramid Lake occurs just prior to 10,810 cal. yr BP and the same sand layer in Bullwinkle layer is radiocarbon dated just prior to 10,750 cal. yr BP. However, regression analysis yields a date of just prior to 7,300 cal. yr BP for Bullwinkle Lake. There is a significant difference between these two dates and suggests that the Bullwinkle Lake chronology and stratigraphic record must be interpreted with caution.

6.2.3 <u>Climate</u>

The midge-inferred temperature reconstruction for Bullwinkle Lake depicts little oscillation with temperatures ranging from 11-13°C in July (Figure 5.9a & 5.9b). Cold-tolerant midge taxa dominate the core, however, warm-adapted taxa are present in greater numbers than they are in Pyramid Lake (Figure 5.8). Midge-inferred mean July air temperatures at Bullwinkle Lake are also higher than in Pyramid Lake, most likely due to the difference in elevation and latitude of the lakes. Pyramid Lake has an elevation of 1,450 m whereas Bullwinkle Lake is located at an elevation of 1,313 m, and Pyramid Lake is approximately 50 km north of Bullwinkle Lake. Pyramid Lake is also deeper and influenced by snowmelt and glaciers at higher elevations.

The corrected mean July air temperature (1971-2000) of 9.8°C does not fit into the range of mean July air temperatures inferred from WA-PLS. A similar problem also occurs in Pyramid Lake and may be an indication that the Beringia training set model is not ideal for this region because it overestimates temperatures.

6.2.3.1 The Early-Middle Holocene

Bullwinkle Lake's palaeoclimatic record starts at 7,300 cal. yr BP. From 7,300-5,100 cal. yr BP (BULL-1) mean July air temperatures rise from a minimum of 11°C to 12.5°C. Species from the subtribe Tanytarsina are the dominant taxa. Tanytarsina are cold stenotherms (Barley et al., 2006) and their presence throughout the core is greatest during the Early-Middle Holocene, when temperatures are the lowest. Other common taxa during this period include *Tanytarsus*, *Psectrocladius (Psectrocladius) sordidellus* type and species from the Tribe Pentaneurini. Both *Cricotopus/Orthocladius* and *Corynoneura/Thienemanniella* are cold-tolerant taxa and are present in moderate abundances when the chronology first begins, during the coldest phase. Shortly after, their presence decreases and remains minimal, but constant throughout the remainder of the core.

Although the signal is not strong, the steady rise in temperature during this period may be an indication of early Holocene warming; however, according to the chronology proposed by the depth-age model, this is not possible. The model gives a basal age of 7,260 cal. yr BP, and the MTM is thought to have occurred in northwestern Canada somewhere between 13,000-10,200 cal. yr BP. If the assumption is made that this model underestimates the true age of the sediments, and inferences are made solely based on the AMS radiocarbon dates, the rise in temperature may fit into the time frame of the MTM. This is because the oldest date obtained from organics found in the Bullwinkle Lake core is 10,750 cal. yr BP.

6.2.3.2 The Middle-Late Holocene

The middle-late Holocene (BULL-2) is characterized by stable temperatures with one minor fluctuation. Tanytarsina has decreased from the early-middle Holocene, and *Corynocera oliveri* type and *Corynocera ambigua* have both increased dramatically. These three taxa dominate and exhibit large fluctuations throughout this period. *Corynocera oliveri* type is typically found in cold, shallow, oligotrophic lakes located above 60°N (Barley, 2004). *Corynocera ambigua* also occurs in cold, shallow, oligotrophic lakes in the arctic and subarctic. Normally it is abundant where it occurs, but in stratigraphic sequences its presence is typically short-lived (Brodersen & Lindegaard, 1999). This is not evident in Bullwinkle Lake, as it is one of the three dominant taxa present from 5,100 cal. yr BP to present. *Tanytarsus* and Pentaneurini both decrease during the transition from the early-middle Holocene to the middle-late Holocene and remain low all through the remainder of the Holocene. *Psectrocladius (Psectrocladius) sordidellus* also stays constant.

From 5,100-1,700 cal. yr BP reconstructed temperatures average 12.5°C. From here, a warming trend occurs until a maximum temperature of just under 13°C is reached at 1,200 cal. yr BP. Temperatures then drop back to 12.5°C by 850 cal. yr BP. During this time, *Corynocera* nr. *ambigua* first appears and fluctuates throughout the remainder of the Holocene. *Corynocera* nr. *ambigua* is also a cold-tolerant species and is typically found in oligotrophic lakes (Porinchu & Cwynar, 2000). It is often confused with *Corynocera ambigua*, due to their similar appearances. In both species the median and first lateral teeth of the mentum form a distinct group that is not on the same focal plane as the outer lateral teeth, which are reduced to one or two teeth. However, *Corynocera ambigua* has median and first lateral teeth that are of a lighter color than the outer lateral teeth, whereas the entire mentum of *Corynocera nr. ambigua* is dark in colour (Brooks et al., 2007).

A similar short-lived increase in temperature during the late Holocene also occurs in Pyramid Lake. Temperatures here begin to warm at 2,750 cal. yr BP, reach their peak at 2,000 cal. yr BP, and then arrive at cooler temperatures by 900 cal. yr BP.

From 900-0 cal. yr BP in Bullwinkle Lake, temperatures remain relatively constant at 12.5°C with few fluctuations.

6.3 Regional Synthesis

The midge-derived reconstructions for Pyramid and Bullwinkle Lakes collectively represent a regional climatic record and contribute to the few palaeoclimatic studies that have been conducted in the western interior mountains of the northwestern Cordillera. To date, no other midge studies have been carried out in northern British Columbia; however, two recent studies using chironomids were conducted in southwestern Yukon

(Barley, 2004) and interior Alaska (Stepanovic, 2006). Often there are inconsistencies in the timing of palaeoclimatic change between maritime and continental interior sites, and this makes them difficult to compare at times. The climate of the northwestern Cordillera is governed by incursions of moist Pacific air that meet dry stable Arctic air masses. The maritime sites are strongly influenced by the Pacific air, whereas sites in the interior mountains are mainly controlled by a continental climate and may yield a different record.

6.3.1 The Early Holocene

Midge-inferred palaeoclimatic reconstructions at Pyramid and Bullwinkle Lakes show similar trends of early Holocene warming. Temperatures reach a maximum of 10.5°C by 8,700 cal. yr BP in Pyramid Lake and a maximum of 12.5°C by 5,600 cal. yr BP in Bullwinkle Lake. Although it appears that this warming may suggest the presence of the MTM, caution should be taken when interpreting the results. The signals at both lakes are not very strong. In addition, the Beringia training-set model may overestimate temperatures at both lakes. Finally, if the ages derived from the depth-age model for Bullwinkle Lake are indeed correct, then the warming trend does not fit into the timing of the MTM found by others. However, if the model underestimates the true age of the sediments, the early Holocene warming may suggest the presence of the MTM at Bullwinkle Lake.

Midge analysis also offers little support for the MTM in southwestern Yukon (Barley, 2004) and interior Alaska (Stepanovic, 2006), (Figure 6.1a, 6.1b, 6.1c & 6.1d). At Antifreeze Pond in the Yukon (Figure 6.1a), Barley (2004) found a cool period from approximately 12,900-9,750 cal. yr BP that coincided with the Younger Dryas, followed

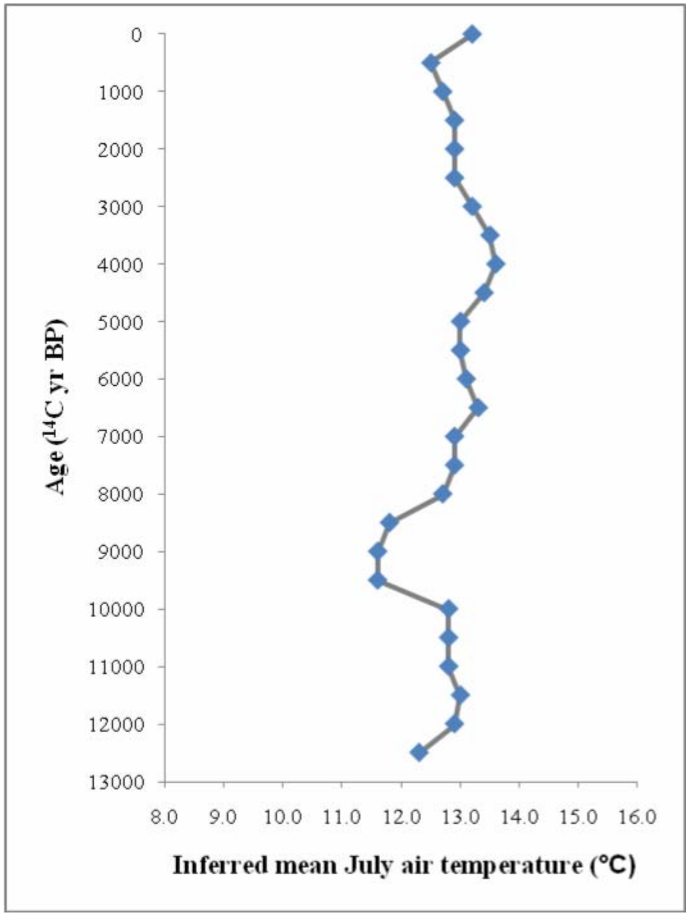

Figure 6.1a: Mean July air temperatures as inferred by WA-PLS as a function of age for Antifreeze Pond, Yukon (Figure 2.1). The temperature curve represents the LOWESS smoothed line (Barley, 2004).

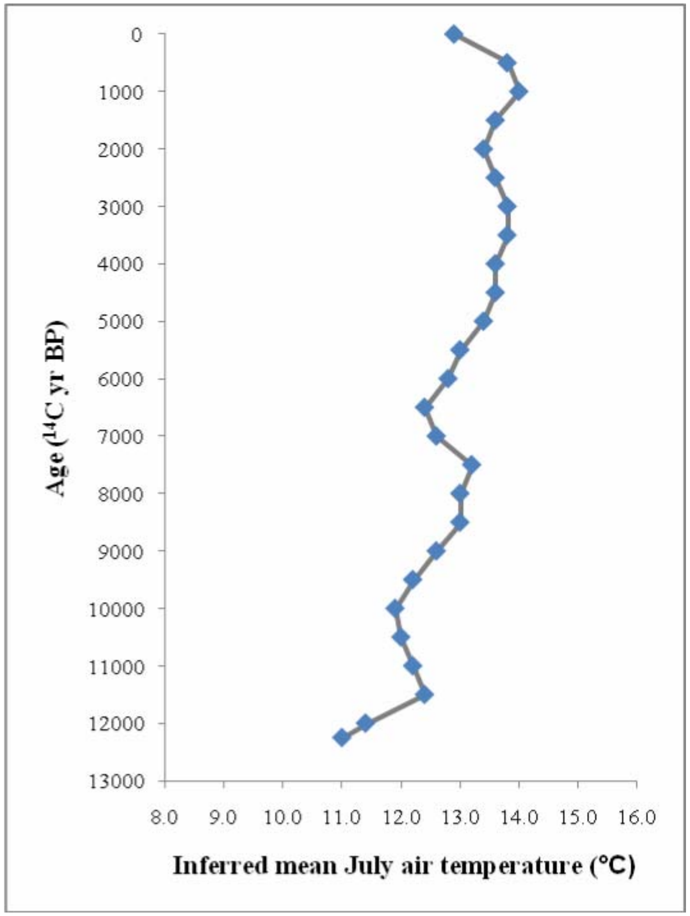

Figure 6.1b: Mean July air temperatures as inferred by WA-PLS as a function of age for Windmill Lake, Alaska (Figure 2.1). The temperature curve represents the LOWESS smoothed line (Stepanovic, 2006).

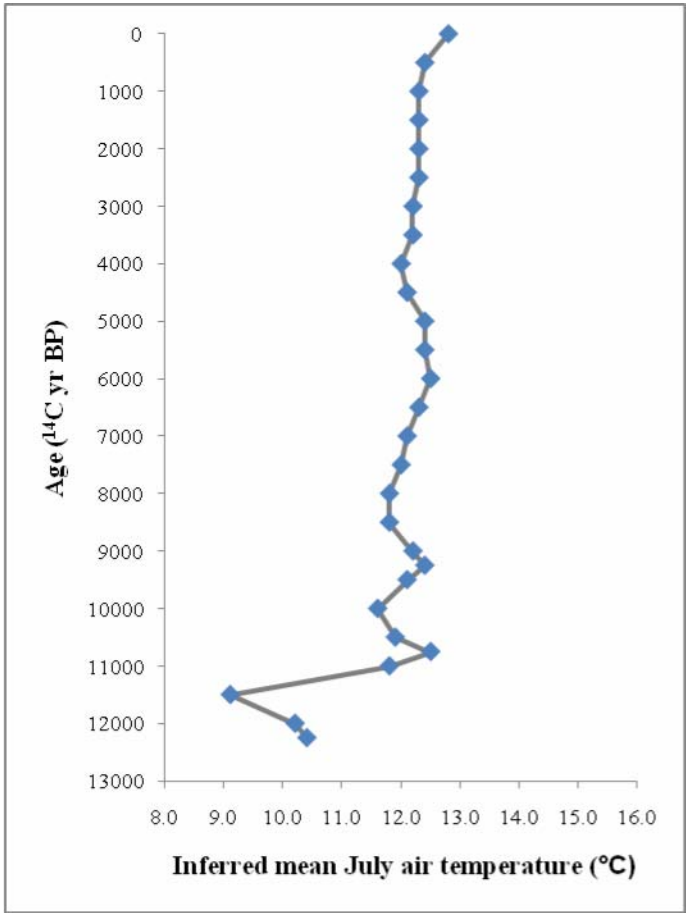

Figure 6.1c: Mean July air temperatures as inferred by WA-PLS as a function of age for Birch Lake, Alaska (Figure 2.1). The temperature curve represents the LOWESS smoothed line (Stepanovic, 2006).

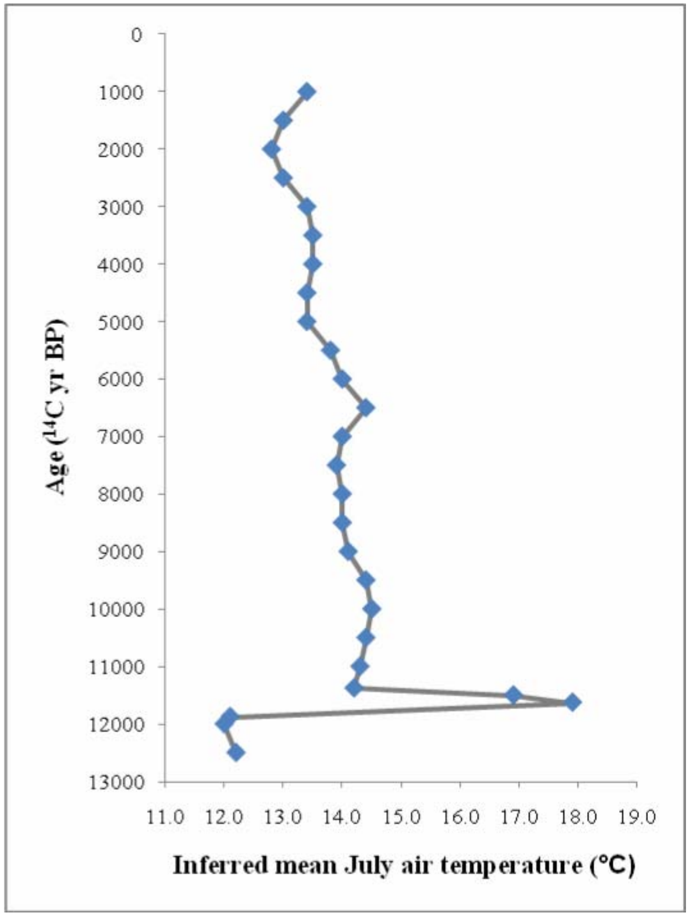

Figure 6.1d: Mean July air temperatures as inferred by WA-PLS as a function of age for Jan Lake, Alaska (Figure 2.1). The temperature curve represents the LOWESS smoothed line (Stepanovic, 2006).

by modern temperatures throughout the rest of the Holocene. At Jan Lake in Alaska (Figure 6.1d), Stepanovic (2006) detected what may have been early Holocene warming, with temperatures peaking at approximately 11,100 cal. yr BP. However this suggestion may be biased due to the high number of *Chaoborus* in the interval. If some other factor, other than temperature, was involved in regulating the abundance of *Chaoborus*, it might yield an erroneous temperature record. The other two lakes included in the study, Windmill and Birch (Figure 6.1b & 6.1c), did not yield any signals for the MTM.

These results contrast with midge analysis in southern British Columbia, which implies a pronounced MTM (Chase et al., 2008; Rosenberg, 2002). Evidence for an early Holocene thermal maximum is strong at Windy Lake in southeastern British Columbia (Chase et al., 2008). Temperatures were 3-4°C warmer than today from 10,500-9,000 cal. yr BP. At Frozen and Eagle Lakes in southern British Columbia, Rosenberg (2002) also detected early Holocene warming at 10,200 cal. yr BP. Other southern British Columbia sites that provide evidence for the MTM include Cabin Lake and 3M Pond. Proposed dates for the event from these locations are 11,400-7,700 cal. yr BP and 11,400-4,500 cal. yr BP, respectively (Walker & Cwynar, 2006).

In general, dates for the MTM in Alaska and northwestern Canada range between 13,000-10,200 cal. yr BP. Several studies conducted in northern British Columbia and surrounding areas have indicated that an early Holocene thermal maximum did occur in the region. However, these studies were based mainly on pollen analysis and geomorphic evidence (Kaufman et al., 2004; Miller & Anderson, 1974; Pisaric et al., 2003; Spooner et al., 1997; Spooner et al, 2002). Perhaps midge analysis has limited abilities to detect such an event which is clearly much weaker than in the southern portion of the province.

Or maybe there are weaknesses in pollen and geomorphic inferences and midge-inferred climates are, in fact, more correct.

Immediately following the inferred early Holocene warming in the Pyramid Lake record is a cooling phase from 8,700-7,900 cal. yr BP. This cold phase is not evident at Bullwinkle Lake; however, a similar event has been recorded at several other sites in the region. Skinny Lake, located to the south of Pyramid Lake in northern British Columbia, exhibited cool and moist conditions from approximately 9,400-7,500 cal. yr BP (Spooner et al., 2002). A cold event was also evident at Windmill and Birch Lake, Alaska (Figure 6.1b & 6.1c) from about 9,750-8,800 and 8,000-7,500 cal yr. BP, respectively (Stepanovic, 2006). These cooling phases all occur around the same time as the 8,200 cal. yr BP cooling event, which lasted close to 200 years and was the most extreme cold episode to occur after the Younger Dryas. Although cooling was centered in the North Atlantic, evidence points to cooling trends at this time all through the western half of the northern hemisphere (Kurek et al., 2004; Pisaric et al., 2003; Shuman et al., 2002; von Grafenstein et al., 1998; Yu & Eicher, 1998). It is clear that this rapid cooling episode occurred at BC2 Lake, in northern British Columbia, at 8,200 cal. yr BP (Pisaric et al., 2003), as well as at Windy Lake, in the southern portion of the province, at 8,250 cal. yr BP (Chase et al., 2008). It is debatable whether the cooling episode at Pyramid Lake is the same cooling event, therefore higher resolution analysis is needed at both Pyramid and Bullwinkle Lakes in order to verify the signal.

6.3.2 The Middle Holocene

Temperatures at Pyramid Lake during the middle Holocene show an overall decrease from around 10-10.5°C to 9.5°C. One minor fluctuation occurs at 7,100 cal. yr

BP, when periods of warming occur and temperatures reach between 10-10.5°C by 5,100 cal. yr BP. From here, a cooling trend occurs into the beginning of the late Holocene. Mazzucchi et al. (2003) found a similar event at Pyramid Lake. Pollen analysis revealed an elevated white spruce (*Picea glauca*) habitat at 5,900 cal. yr BP, which supported the idea of several high-magnitude rainstorm events resulting from increased summer temperatures. This warm period lasted until 4,500 cal. yr BP. Warm periods during the middle Holocene have also been recorded at Susie Lake (Spooner et al., 1997) and BC2 Lake (Pisaric et al., 2003) in northern British Columbia, in addition to several lakes on a transect from Juneau, Alaska to Altin, British Columbia (Miller & Anderson, 1974).

The overall cooling trend at Pyramid Lake, minus the short warm interval, is also reflected in the midge record (Figure 6.1d) from Jan Lake, Alaska (Stepanovic, 2006). Regional cooling was also recorded at Skinny Lake, British Columbia (Spooner et al., 2002) and a middle Neoglacial advance occurred in the northern Coast Mountains of the province around 2,800 cal. yr BP (Clague & Mathewes, 1996). Windy (Chase et al., 2008), Frozen and Eagle Lakes (Rosenberg, 2002) in southern British Columbia also displayed decreasing temperatures during the middle Holocene. This trend is widely documented in western North America (Hebda, 1995; Walker & Pellatt, 2003) and is consistent with a decrease in summer insolation from approximately 6,000-4,000 cal. yr BP (Chase et al., 2008).

Midge analysis from Bullwinkle Lake reveals a slightly different trend. From 5,070-1,700 cal. yr BP temperatures fluctuate little and remain an average of 12.5°. A similar climate is seen at Antifreeze Pond in southwestern Yukon (Figure 6.1a), where temperatures are at modern and vary little throughout the middle and late Holocene (Barley, 2004).

6.3.3 <u>The Late Holocene</u>

Changes in regional air-mass circulation patterns related to the Aleutian Low resulted in a late Holocene climate differing from the middle Holocene (Spooner et al., 2002). Changes in vegetation, due to the dispersal of coastal pollen towards the eastern portions of the province, were noted at several sites in the interior (Spear & Cwynar, 1997; Spooner et al., 2002), including Pyramid Lake (Mazzucchi et al., 2003). At Pyramid Lake, midge-inferred temperatures cooled to modern temperatures by 3,900 cal. yr BP. At 2,750 cal. yr BP, a warming occurred until temperatures reached 10.5°C at 1,970 cal. yr BP. Cooling then occurred and temperatures reached 9.5°C, slightly above modern, by 900 cal. yr BP. A similar trend also occurs in Bullwinkle Lake. Beginning at 1,700 cal. yr BP, temperatures increase to just below 13°C by 1,200. From here, the area cools until a temperature of 12.5° is reached at 900 cal. yr BP. Temperatures remained the same with few fluctuations until present. The Little Ice Age (LIA), the most recent glacier expansion event of the late Holocene is not apparent in either lake. Perhaps higher resolution analysis during this period will yield a clearer signal.

Cooler conditions, indicative of the LIA, were evident at several sites in the northern part of the province, including Drizzle Pond, Waterdevil Lake (Spear & Cwynar, 1997), Summit Lake (Clague & Mathewes, 1996) and Spillway Pond (Clague & Mathewes, 1996). However, midge analysis from lakes in Yukon and Alaska (Figure 6.1a, 6.1b, 6.1c & 6.1d), like Pyramid and Bullwinkle Lakes, had no clear record of this cooling event (Barley, 2004; Stepanovic, 2006).

Chapter VII

CONCLUSIONS

- Pyramid and Bullwinkle Lake's records for the Holocene provide the first midge-inferred mean July air temperatures for northern British Columbia.
- The Holocene temperature reconstruction for Pyramid Lake depicts oscillating temperatures, ranging from 8.5-10.5°C, whereas the reconstruction from Bullwinkle Lake reveals little fluctuation, with temperatures ranging from 11-13°C. Cold-tolerant midge taxa dominate the cores from both Pyramid and Bullwinkle Lakes; however, warm-adapted species are more common in Bullwinkle Lake.
- Early Holocene warming is evident in both Pyramid and Bullwinkle Lake's records. Temperatures in Pyramid Lake reached a maximum of 10.5°C at 8,700 cal. yr BP and reached 12.5°C in Bullwinkle Lake at 5,600 cal. yr BP. It is unclear whether these temperatures are indicative of the Milankovitch Thermal Maximum (MTM). Midge analysis in southwestern Yukon (Barley, 2004) and interior Alaska (Stepanovic, 2006) offer little support for an early Holocene warm interval. These results contrast with studies performed in southern British Columbia, where midge analysis revealed a pronounced MTM (Chase et al., 2008; Rosenberg, 2002).
- From 8,700-7,900 cal. yr BP, a cooling phase is apparent at Pyramid Lake. This occurs about when the 8,200 cal. yr BP cooling event occurred in the northern hemisphere. Higher resolution analysis is needed on this section of the core to determine if the signal is actually related to this event.
- During the middle Holocene, records from Pyramid Lake indicate an overall decrease in temperatures; however, a short warming interval is apparent when temperatures

reached between 10-10.5°C at 5,100 cal. yr BP. Mazzucchi et al. (2003) had similar results at the lake using pollen analysis.

- Inferred temperatures at Bullwinkle Lake during the middle Holocene fluctuate little, and average 12.5°C.
- A similar short warming phase during the late Holocene occurs in the reconstructions from both Pyramid and Bullwinkle Lake. Temperatures peak at 2,000 cal. yr BP (10.5°C) in Pyramid Lake and at 1,200 cal. yr BP (13°C) in Bullwinkle Lake. From here, temperatures cool to 9.5°C, just above modern, by 900 cal. yr BP in Pyramid Lake and to 12.5°C by 850 cal. yr BP in Bullwinkle Lake.
- The Beringia training-set model appears to overestimate temperatures at both Pyramid and Bullwinkle Lake, and therefore may not be ideal for this region. Perhaps additional lakes should be added to the model to represent the area better, or maybe an entirely separate model is required for the northern interior of British Columbia.
- Several inversions are apparent in the AMS radiocarbon dates from Bullwinkle Lake. These may be caused by the hard-water effect or old carbon contamination, which would yield older-than-expected dates. Increased sediment mixing and resuspension of dating materials caused by shallow waters and the lake's location in a wind corridor may have also caused the inversions. In addition, changes in the lake's size throughout the Holocene, likely caused by beaver activity, might have altered the water's geochemistry and may be reflected in the AMS radiocarbon dates.
- The depth-age model proposed for Bullwinkle Lake appears to underestimate the true age of the sediments; therefore, its chronology may not be entirely accurate.

- A pyroclastic sand deposit is present in both Pyramid and Bullwinkle Lakes. It occurs at approximately 10,810 cal. yr BP in Pyramid Lake and at approximately 10,750 in Bullwinkle Lake. The material resembles other deposits in lakes near Dease Lake and Finlay River in northern British Columbia. Possible sources for the pyroclastic sand are located in the Stikine Volcanic Belt and include Mount Edziza, Hoodoo Mountain, Heart Peaks and Level Mountain (Lakeman, 2006). Additional research in the region is required to isolate the location of the eruption.
- Midge-inferred Holocene temperatures from Pyramid and Bullwinkle Lakes support the value of midges as a proxy for climate. Further high-resolution midge analysis is required in the area to produce a more detailed reconstruction of both the large magnitude and subtle temperature fluctuations throughout the Holocene.

REFERENCES

Alley, R.B., P.A. Mayewski, T. Sowers, M. Stuiver, K.C. Taylor and P.U. Clark. (1997). Holocene climatic instability: a prominent, widespread event 8200 yr ago. Geology. 25: 483-486.

Armitage, P., P.S. Cranston and L.C.V. Pinder. (1995). The Chironomidae: The biology and ecology of non-biting midges. Chapman and Hall, London. 572 pp.

Banner, A., J. Pojar and G.E. Rouse. (1983). Postglacial paleoecology and successional relationships of Bog woodland near Prince Rupert, British Columbia. Canadian Journal of Forest Research. 13: 938-947.

Barley, E.M. (2004). Paleoclimate analysis of southwestern Yukon Territory using subfossil chironomid remains from Antifreeze Pond. M.Sc. Thesis, Simon Fraser University, Burnaby, Canada.

Barley, E.M., I.R. Walker, J. Kurek, L.C. Cwynar, R.W. Mathewes, K. Gajewski and B.P. Finney. (2006). A northwest North American training set: distribution of freshwater midges in relation to air temperature and lake depth. Journal of Paleolimnology.

Berger, A. and M.F. Loutre. (1991). Insolation values for the climate of the last 10 million years. Quaternary Science Reviews. 10: 297-317.

Bjorck, S., B. Kromer, S. Johnsen, O. Bennike, D. Hammarlund, G. Lemdahl, G. Possnert, T.L. Rasmussen, B. Wohlfarth, C.U. Hammar and M. Spurk. (1996). Synchronized terrestrial-atmospheric deglacial records around the North Atlantic. Science. 274: 1155-1160.

Bjorck, S., M. Rundgren, O. Ingolfsson and S. Funder. (1997). The Preboreal Oscillation around the Nordic Seas: terrestrial and lacustrine responses. Journal of Quaternary Science. 12: 455-465.

Bond, G., B. Kromer, J. Beer, R. Muscheler, M.N. Evan, W. Showers, S. Hoffmann, R. Lotti-Bond, I. Hajdas and G. Bonani. (2001). Persistent solar influence on North Atlantic climate during the Holocene. Science. 294: 2130-2136.

Bradley, R.S. (1999). Paleoclimatology: Reconstructing Climates of the Quaternary. Academic Press, California. 613 pp.

Brodersen, K.P. and C. Lindegaard. (1999). Mass occurrence and sporadic distribution of *Corynocera ambigua* Zetterstedt (Diptera, Chironomidae) in Danish lakes. Neo and palaeolimnological records. Journal of Paleolimnology. 22: 41-52.

Brooks, S.J. and H.J.B Birks. (2000). Chironomid-inferred late-glacial and early-Holocene mean July air temperatures for Krakenes Lake, western Norway. Journal of Paleolimnology. 23: 77-89.

Brooks, S.J., P.G. Langdon and O. Heiri. (2007). The identification and use of Palaearctic Chironomidae larvae in palaeoecology. Quaternary Research Association, London. 276 pp.

Calkin, P.E., G.C. Wiles and D.J. Barclay. (2001). Holocene coastal glaciation of Alaska. Quaternary Science Reviews. 20: 449-461.

Chase, M., C. Bleskie, I.R. Walker, D.G. Gavin and F.S. Hu. (2008). Midge-inferred Holocene summer temperatures in southeastern British Columbia, Canada. Palaeogeography, Palaeoclimatology, Palaeoecology. 257: 244-259.

Clague, J.J. (1984). Quaternary geology and geomorphology, Smithers-Terrace-Prince Rupert area, British Columbia. Geological Survey of Canada Memoir. 413: 71pp.

Clague, J.J. and R.W. Mathewes. (1996). Neoglaciation, glacier-dammed lakes and vegetation change in northwestern British Columbia, Canada. Arctic and Alpine Research. 28: 10-24.

Crowley, T.J. (2000). Causes of climatic change over the past 1000 years. Science. 289: 270-277.

Cwynar, L.C. (1993). The abundance of exotic western hemlock pollen at Waterdevil Lake, White Pass, northern British Columbia: a preliminary analysis. Review of Palaeobotany and Palynology. 79: 113-119.

Cwynar, L.C., R.W. Spear, J. Vincent and J. Kurek. (2003). The Preboreal Oscillation in eastern North America. Joint Annual Meeting of the Canadian Quaternary Association and the Canadian Geomorphology Research Group.

Dean, W.E. (1974). Determination of carbonate and organic matter in calcareous sediments and sedimentary rocks by loss on ignition: comparison with other methods. Journal of Sedimentary Petrology. 44: 242-248.

Dean, W.E., R.M. Forester and J.P. Bradbury. (2002). Early Holocene change in atmospheric circulation in the Northern Great Plains: an upstream view of the 8.2 ka cold event. Quaternary Science Reviews. 21: 1763-1775.

Dixon-Warren, A.B. and A.S. Hickin. (2000). Ancient Pacific Margin Natmap Part IV: surficial mapping and till geochemistry in the Swift River area, northwestern British Columbia. In Geological Fieldwork, 1999 British Columbia Ministy of Energy and Mines Paper. 2000-1: 47-69.

Dyke, A.S. (2006). Late Quaternary vegetation history of northern North America based on pollen, macrofossil and faunal remains. Geographie Physique et Quaternaire. 59: 211-262.

Environment Canada. (2008). Canadian climate normals (1971-2000). National Climate Data and Information Archive.

Fisher, T.G. and D.G. Smith. (1994). Glacial Lake Agassiz: its northwest maximum extent and outlet in Saskatchewan (Emerson phase). Quaternary Science Reviews. 13: 845-858.

Fisher, T.G., D.G. Smith and J.T. Andrews. (2002). Preboreal Oscillation cause by a glacial Lake Agassiz flood. Quaternary Science Reviews. 21: 873-878.

Gilbert, R and J. Glew. (1985). A portable percussion coring device for lacustrine and marine sediments. Journal of Sedimentary Petrology. 55: 607-608.

Glew, J.R. (1989). A new trigger mechanism for sediment samplers. Journal of Paleolimnology. 2: 241-243.

Gottesfeld, A.S., R.W. Mathewes and L.M.J. Gottesfeld. (1991). Holocene debris flows and environmental history, Hazelton area, British Columbia. Canadian Journal of Earth Science. 28: 1583-1593.

Grimm, E.C. (1993). TILIA version 2.0.b.4. Illinois State Museum.

Grimm, E.C. (2004). TGView version 2.0.2. Illinois State Museum.

Grove, J.M. (2001). The initiation of the “Little Ice Age” in regions round the North Atlantic. Climatic Change. 48: 53-82.

Hald, M. and S. Hagen. (1998). Early Preboreal cooling in the Nordic seas region triggered by meltwater. Geology. 26: 615-618.

Hammarlund, D., S. Bjorck, B. Buchardt and C.T. Thomsen. (2005). Limnic responses to increased effective humidity during the 8200 cal. yr BP cooling event in southern Sweden. Journal of Paleolimnology. 34: 471-480.

Harris, S.A. (2002). Global heat budget, plate tectonics and climate change. Geografiska Annaler Series A: Physical Geography. 1: 1-9.

Hebda, R.J. (1995). British Columbia vegetation and climate history with focus on 6 ka BP. Geographie Physique et Quaternaire. 49: 55-79.

Heiri, O. (2004). Within-lake variability of subfossil chironomid assemblages in shallow Norwegian lakes. Journal of Paleolimnology. 00: 1-18.

Heiri, O., H.J.B. Birks, S.J. Brooks, G. Velle and E. Willassen. (2003). Effects of within-lake variability of fossil assemblages on quantitative chironomid-inferred temperature reconstruction. Palaeogeography, Palaeoclimatology, Palaeoecology. 3173: 1-12.

Hoffmann, W. (1986). Chironomid Analysis. In: B.E. Berglund (ed.) Handbook of Holocene Palaeoecology and Palaeohydrology. John Wiley & Sons, Chichester. 715-727.

Imbrie, J. and J.Z. Imbrie. (1980). Modeling the climatic response to orbital variations. Science. 207: 943-953.

Johnson, S., H.B. Clausen, W. Dansgaard, N.S. Gundestrup, M. Hansson, P. Johnsson, P. Steffensen and A.E. Sveinbjornsdottir. (1992). A deep ice core from east Greenland. Geoscience. 29: 22 pp.

Juggins, S. (2003-2006). C2 version 1.4.3. University of Newcastle.

Karrow, P.F. and T.W. Anderson. (1975). Palynological study of lake sediment profiles from southwestern New Brunswick; discussion. Canadian Journal of Earth Sciences. 12: 1808-1812.

Kaufman, D.S., T.A. Ager, N.J. Anderson, P.M. Anderson, J.T. Andrews, P.J. Bartlein, L.B. Brubaker, L.L. Coats, L.C. Cwynar, M.L. Duvall, A.S. Dyke, M.E. Edwards, W.R. Eisner, K. Gajewski, A. Geirsdottir, F.S. Hu, A.E. Jennings, M.R. Kaplan, M.W. Kerwin, L.V. Lozhkin, G.M. MacDonald, G.H. Miller, C.J. Mock, W.W. Oswald, B.L. Otto-Bleisner, D.F. Porinchu, K. Ruhland, J.P. Smol, E.J. Steig and B.B. Wolfe. (2004). Holocene thermal maximum in the western Arctic (0-180ºW). Quaternary Science Reviews. 23: 529-560.

Klitgaard-Kristensen, D., H.P. Sejrup, H. Haflidason, S. Johnsen and M. Spurk. (1998). A regional 8200 cal. yr BP cooling event in northwest Europe, induced by final stages of the Laurentide ice-sheet deglaciation? Journal of Quaternary Science. 13: 165-169.

Kurek, J., L.C. Cwynar and R.W. Spear. (2004). The 8200 cal yr BP cooling event in eastern North America and the utility of midge analysis for Holocene temperature reconstructions. Quaternary Science Reviews. 23: 627-639.

Lakeman, T.R. (2006). Late-glacial alpine glacier advance and early Holocene tephras, northern British Columbia. M.Sc. Thesis, Simon Fraser University, Burnaby, Canada.

Larocque, I. and R.I. Hall. (2003). Chironomids as quantitative indicators of mean July air temperature: validation by comparison with century-long meteorological records from northern Sweden. Journal of Paleolimnology. 29: 475-493.

Larocque, S.J. and D.J Smith. (2003). Little Ice Age glacial activity in the Mt. Waddington area, British Columbia Coast Mountains, Canada. Canadian Journal of Earth Sciences. 40: 1413-1436.

Lewis, D.H. and D.J. Smith. (2004). Little Ice Age glacial activity in Strathcona Provincial Park, Vancouver Island, British Columbia, Canada. Canadian Journal of Earth Sciences. 41: 285-297.

Lotter, A.F., I.R. Walker, S.J. Brooks and W. Hofmann. (1999). An intercontinental comparison of chironomid palaeotemperature inference models: Europe vs. North America. Quaternary Science Reviews. 18: 717-735.

Luckman, B.H. (1994). Using multiple high-resolution proxy climate records to reconstruct natural climate variability: an example from the Canadian Rockies. Mountain Environments and Changing Climates. London and New York. 42-59.

Luckman, B.H. (1995). Calendar-dated, early "Little Ice Age" glacier advance at Robson Glacier, British Columbia, Canada. The Holocene. 5: 149-159.

Luckman, B.H. (2000). The Little Ice Age in the Canadian Rockies. Geomorphology. 32: 357-384.

MacDonald, G.M. (1984). Postglacial plant migration vegetation development in the western Canadian boreal forest. Ph.D. Thesis, University of Toronto.

MacDonald, G.M. (1987). Postglacial development of the subalpine-boreal transition forest of western Canada. Journal of Ecology. 75: 303-320.

MacDonald, G.M. and L.C. Cwynar. (1985). A fossil pollen based reconstruction of the late Quaternary history of lodgepole pine (*Pinus contorta* ssp. *latifolia*) in the western interior of Canada. Canadian Journal of Forest Research. 15: 1039-1044.

MacDonald, G.M., R.P. Beukens and W.E. Kieser. (1991). Radiocarbon dating of limnic sediments: A comparative analysis and discussion. Ecology. 72: 1150-1155.

McCuaig, S.J. and M.C. Roberts. (2002). Topographically-independent ice flow in northwestern British Columbia: implications for Cordilleran ice sheet construction. Journal of Quaternary Science. 17: 341-348.

Magny, M., C. Begeot, J. Guiot and O. Peyron. (2003). Contrasting patterns of hydrological changes in Europe in response to Holocene climatic cooling phases. Quaternary Science Reviews. 22: 1589-1596.

Mazzucchi, D. (2000). Holocene environmental reconstruction of the Cassiar Region, northwestern British Columbia. M.Sc. Thesis, Queen's University, Kingston, Canada.

Mazzucchi, D., I.S. Spooner, R. Gilbert and G. Osborn. (2003). Reconstruction of Holocene climate change using multiproxy analysis of sediments from Pyramid Lake, British Columbia, Canada. Arctic, Antarctic and Alpine Research. 35: 520-529.

Milankovitch, M. (1941). Canon of insolation and the Ice Age problem. Royal Academy of Serbia. 133: 633 pp.

Miller, M.M. and J.H. Anderson. (1974). Out-of-phase Holocene climate trends in the maritime and continental sectors of the Alaska-Canada boundary range. Quaternary Environments: Proceedings of a Symposium. York University Geographical Monographs. 5: 33-58.

O'Brian, S.R., P.A. Mayewski, L.D. Meeker, M.S. Twickler and S.I. Whitlow. (1995). Complexity of Holocene climate as reconstructed from a Greenland ice core. Science. 270: 1962-1964.

Oliver, D.R. and M.E. Roussel. (1983). The insects and arachnids of Canada. Part 11. The genera of larval midges of Canada; Diptera: Chironomidae. Agriculture Canada Publication. 1746: 263 pp.

Palmer, S.L., I.R. Walker, M.L. Heinrichs, R. Hebda and G. Scudder. (2002). Postglacial midge community change and Holocene palaeotemperature reconstructions near treeline, southern British Columbia (Canada). Journal of Palaeolimnology. 28: 469-490.

Pilgrim, L. (1904). Versuch einer rechnerischen behandlung des eiszeitenproblems. Jahreshefte fur vaterlandische Naturkunde in Wurttemberg. 60.

Pisaric, M.F.J., C. Holt, J.M. Szeicz, T. Karst and J.P Smol. (2003). Holocene treeline dynamics in the mountains of northeastern British Columbia, Canada, inferred from fossil pollen and stomata. The Holocene. 13: 161-173.

Plouffe, A. and V.M. Levson. (2001). Late Quaternary glacial and interglacial environments of the Nechako River-Cheslatta Lake area, central British Columbia. Canadian Journal of Earth Science. 38: 719-731.

Polissar, P.J., M.B. Abbott, A.P. Wolfe, M. Bezada, V. Rull and R.S. Bradley. (2006). Solar modulation of Little Ice Age climate in the tropical Andes. PNAS. 103: 8937-8942.

Porinchu, D.F. and L.C. Cwynar. (2000). The distribution of freshwater Chironomidae (Insecta: Diptera) across treeline near the Lower Lena River, northeast Siberia, Russia. Arctic, Antarctic and Alpine Research. 32: 429-437.

Reasoner, M.A. (1993). Equipment and procedure improvements for a lightweight, inexpensive percussion core sampling system. Journal of Paleolimnology. 8: 291-316.

Reyes, A.V., B.H. Luckman, D.J. Smith, J.C. Clague and R.D. van Dorp. (2006). Tree-ring dates for the maximum Little Ice Age advance of Kaskawulsh Glacier. Arctic. 59: 14-20.

Ritchie, J.C. (1985). Late-Quaternary climatic and vegetational change in the lower Mackenzie basin, northwest Canada. Ecology. 66: 612-621.

Rosenberg, S.M. (2002). Holocene palaeoenvironmental records from two subalpine lakes in southern British Columbia, based on chironomid and pollen analysis. M.Sc. Thesis, Simon Fraser University, Burnaby, Canada.

Rosenberg, S.M., I.R. Walker, R.W. Mathewes and D.J. Hallett. (2004). Midge-inferred Holocene climate history of two subalpine lakes in southern British Columbia, Canada. Holocene. 14: 258-271.

Ryder, J.M. and D. Maynard. (1991). The Cordilleran Ice Sheet in northern British Columbia. Geographie Physique et Quaternaire. 45: 355-363.

Shotton, F.W. (1972). An example of hard-water error in radiocarbon dating of vegetable matter. Nature. 240: 460-461.

Shuman, B., P. Bartlein, N. Logar, P. Newby and T. Webb III. (2002). Parallel climate and vegetation responses to the early Holocene collapse of the Laurentide Ice Sheet. Quaternary Science Reviews. 21: 1793-1805.

Smith, D.J. and J.R. Desloges. (2000). Little Ice Age history of Tzeetsaytsul Glacier, Tweedsmuir Provincial Park, British Columbia. Geographie Physique et Quaternaire. 54: 135-141.

Spear, R.W. and L.C. Cwynar. (1997). Late Quaternary vegetation history of White Pass, northern British Columbia, Canada. Arctic and Alpine Research. 29: 45-52.

Spooner, I.S. and G.D. Osborn. (2000). Geomorphology and Late Wisconsinan sedimentation in the Stikine River valley, northern British Columbia. Quaternary International. 68-71: 285-296.

Spooner, I.S., L.V. Hills and G.D. Osborn. (1997). Reconstruction of Holocene changes in alpine vegetation and climate, Susie Lake, British Columbia, Canada. Arctic and Alpine Research. 29: 156-163.

Spooner, I.S., D. Mazzucchi, G. Osborn, R. Gilbert and I. Larocque. (2002). A multi-proxy record of environmental change from the sediments of Skinny Lake, Iskut Region, northern British Columbia, Canada. Journal of Paleolimnology. 28: 419-431.

Spooner, I.S., S. Barnes, K.B. Baltzer, R. Raeside, G.D. Osborn and D. Mazzucchi. (2003). The impact of air mass circulation dynamics on Late Holocene paleoclimate in northwestern North America. Quaternary International. 108: 77-83.

Stepanovic, L.C. (2006). 12 500 years of midge-inferred climatic history for interior Alaska. M.Sc. Thesis, Simon Fraser University, Burnaby, Canada.

Stuart, G.S.L., J.W. Helmer and L.V. Hills. (1989). The Holocene paleoecology of Jenny Lake area, southwest Yukon, and its implications for prehistory. Arctic. 42: 347-353.

Stuiver, M. and P.J. Reimer. (1986-2008). CALIB REV5.0.2.

Stumpf, A.J, B.E. Broster and V.M. Levson. (2000). Multiphase flow of the late Wisconsinan Cordilleran ice sheet in western Canada. GSA Bulletin. 112: 1850-1863.

Tallman, A.M. (1975). Glacial and periglacial geomorphology of the Fourth of July Creek valley, Atlin Region, Cassiar District, northwestern British Columbia. PhD Thesis. Michigan State University.

Teller, J.T., D.W. Leverington and J.D. Mann. (2002). Freshwater outbursts to the oceans from glacial Lake Agassiz and their role in climate change during the last deglaciation. Quaternary Science Reviews. 21: 879-887.

ter Braak, C.F.J., S. Juggins, H.J.B Birks and van der Voet, H. (1993). Weighted averaging partial least squares regression (WA-PLS): definition and comparison with other methods for species-environment calibration. In G.P. Patil and C.R. Rao (eds), Multivariate Environmental Statistics. Elsevier, Amsterdam. 35 pp.

von Grafenstein, U., H. Erlenkeuser, J. Muller, J. Jouzel and S. Johnsen. (1998). The cold event 8200 years ago documented in oxygen isotope records of precipitation in Europe and Greenland. Climate Dynamics. 14: 73-81.

Waddington, J.C.B. (1969). A stratigraphic record of the pollen influx to a lake in the Big Woods of Minnesota. Geological Society of America Special Paper. 123: 263-282.

Wagner, F., S.J.P. Bohncke, D.L. Dilcher, W.M. Kurschner, B. van Geel and H. Visscher. (1999). Century-scale shifts in early Holocene atmospheric CO_2

concentration. Science. 284: 1971-1973.

Walker, I.R. (1987). Chironomidae (Diptera) in paleoecology. Quaternary Science Reviews. 6: 29-40.

Walker, I.R. (2001). Midges: Chironomidae and related Diptera. In J.P. Smol, H.J.B. Birks and W.M. Last (eds), Tracking Environmental Change using Lake Sediments, Volume 4, Zoological Indicators. Kluwer Academic Publishers, Dordrecht. pp. 43-66.

Walker, I.R. and L.C. Cwynar. (2006). Midges and palaeotemperature reconstruction – The North American experience. Quaternary Science Reviews. 25: 1911-1925.

Walker, I.R. and M.G. Pellatt. (2003). Climate change in coastal British Columbia – A paleoenvironmental perspective. Canadian Water Resources Journal. 28: 531-566.

Walker, I.R., R.J. Mott and J.P. Smol. (1991). Allerod-Younger Dryas lake temperatures from midge fossils in Atlantic Canada. Science. 253: 1010-1012.

White, J.M. and R.W. Mathewes. (1982). Holocene vegetation and climate changes in the Peace River district, Canada. Canadian Journal of Earth Science. 19: 555-570.

Wright, H.E., Jr. (1967). A square-rod piston sampler for lake sediments. Journal of Sedimentary Petrology. 37: 957-976.

Yu, Z. (2000). Ecosystem response to late-glacial and early Holocene climate oscillations in the Great Lakes region of North America. Quaternary Science Reviews. 19: 1723-1747.

Yu, Z. and H.E. Wright, Jr. (2001). Response of interior North America to abrupt climate oscillations in the North Atlantic region during the last deglaciation. Earth-Science Reviews. 52: 333-369.

Yu, Z. and U. Eicher. (1998). Abrupt climate oscillations during the last deglaciation in central North America. Science. 282: 2235-2238.